JOC Article

Syntheses and Reactivity of *meso*-Unsubstituted Azuliporphyrins Derived from 6-*tert*-Butyl- and 6-Phenylazulene†

Timothy D. Lash,* Jessica A. El-Beck, and Gregory M. Ferrence

Department of Chemistry, Illinois State University, Normal, Illinois 61790-4160

tdlash@ilstu.edu

Received July 23, 2007

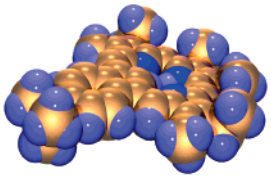

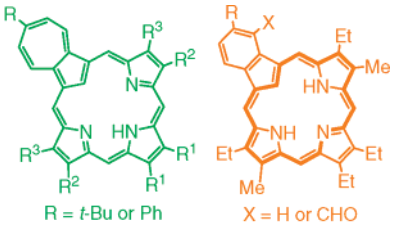

A series of six azuliporphyrins with substituents on the seven-membered ring were prepared by two different "3 + 1" routes from 6-*tert*-butyl- and 6-phenylazulene. The substituted azulenes can be converted into dialdehydes under Vilsmeier−Haack conditions, and these react with tripyrranes in the presence of TFA in CH_2Cl_2 to give azuliporphyrins in excellent yields. Alternatively, tripyrrane analogues can be prepared by reacting the substituted azulenes with an acetoxymethylpyrrole in the presence of acetic acid, and following a deprotection step, these condensed with a pyrrole dialdehyde to give the related azuliporphyrins in 45−51% yield. Five of the azuliporphyrins were sufficiently soluble in $CDCl_3$ to afford high-quality proton and carbon-13 NMR data. The internal CH and NH resonances were observed near 3 ppm, although the precise values were dependent upon substituent effects. The presence of a *tert*-butyl group on the azulene moiety slightly enhanced the diatropicity of the macrocycle compared to the phenyl-substituted azuliporphyrins. Polar solvents also increased the downfield shifts to the external protons by stabilizing the dipolar resonance contributors that are responsible for the carbaporphyrinoid aromatic character. A *tert*-butyl-substituted azuliporphyrin also gave X-ray quality crystals, and this allowed the first structural analysis of a free base azuliporphyrin to be conducted. The macrocycle is near planar, and the azulene unit was only tilted out of the plane by 7.4°. An analysis of the bond lengths suggests that a 17 atom delocalization pathway significantly contributes to the aromatic properties of this system. Protonation of azuliporphyrins affords dications with enhanced diamagnetic ring currents where the internal CH shifts to ca. −3 ppm. Again, the chemical shifts are influenced by the substituents and the presence of an electron-donating *tert*-butyl group on the azulene subunit increases the macrocyclic diatropicity. Two of the substituted azuliporphyrins were reacted with nickel(II) acetate or palladium(II) acetate in DMF to give the corresponding organometallic derivatives, and these stable complexes were isolated in excellent yields. Addition of pyrrolidine to NMR solutions of 2^3-substituted azuliporphyrins **19** demonstrated that nucleophilic addition products were present in equilibrium with the parent porphyrinoids, but these adducts are less favored than for azuliporphyrins lacking the 2^3-substituents. Although nucleophilic attack of a peroxide anion is believed to be the first step in the conversion of azuliporphyrins to benzocarbaporphyrins with *t*-BuOOH and KOH, the *tert*-butyl or phenyl substituents in azuliporphyrins **19a** and **19b** did not inhibit this chemistry. Two benzocarbaporphyrin products were isolated and characterized in each case, and mechanisms are proposed to explain the origins of these oxidative ring contraction products.

Introduction

Porphyrin analogues with carbocyclic rings in place of one of the usual pyrrole units can be synthesized by reacting dialdehydes with tripyrrolic intermediates (tripyrranes) using the "3 + 1" variant of the MacDonald condensation.[1−3] Using this approach, carbaporphyrinoid systems such as **1**−**4** (Chart 1)[4−7]

* To whom correspondence should be addressed.

† Conjugated Macrocycles Related to the Porphyrins. 45. For part 44, see: El-Beck, J. A.; Lash, T. D. *Eur. J. Org. Chem.* **2007**, 3981-3990.

(1) Lash, T. D. *Chem. Eur. J.* **1996**, *2*, 1197−1200.
(2) Lash, T. D. *Synlett* **2000**, 279−295.

10.1021/jo701523s CCC: $37.00
Published on Web 10/05/2007

CHART 1

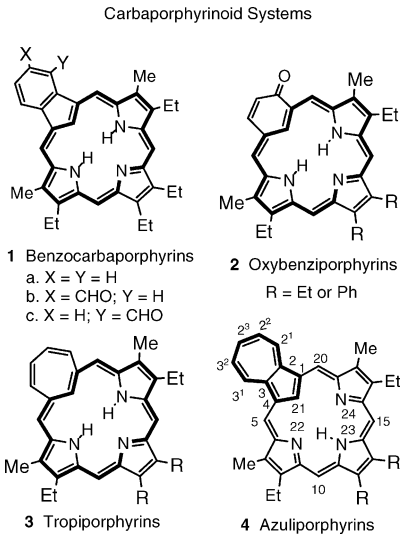

with diverse chemical and spectroscopic properties are easily prepared. Although benzocarbaporphyrins **1** and oxybenziporphyrins **2** have strongly diatropic characteristics that are comparable to true porphyrins,[4,5] this property is reduced in tropiporphyrins **3** due to distortions resulting from the presence of a seven-membered ring.[6] Azuliporphyrins **4** have even smaller diatropic ring currents that result from cross-conjugation by the azulene subunit.[7,8] This factor seems to be overcome to a certain extent by dipolar canonical forms such as **4′** that give the system tropylium ion character while simultaneously allowing for a carbaporphyrinoid 18π electron delocalization pathway (Scheme 1).[7,8] However, the effect is limited due to the associated need for charge separation. Addition of acid leads to diprotonation and the resulting dications **4**H_2^{2+} show greatly enhanced diatropicity where the internal CH resonance shifts upfield to ca. −3 ppm (Scheme 1).[7,8] This increased aromatic character is attributed to an increased favorability for resonance structures such as **4′**H_2^{2+} which now aid in charge delocalization.[7,8]

Azuliporphyrins readily form organometallic derivatives with nickel(II), palladium(II), and platinum(II) salts,[9,10] and these metalation reactions closely parallel results obtained for N-confused porphyrins.[11,12] This system also undergoes an unusual oxidative metalation reaction with copper(II) salts,[13] and treatment of **4a** with peroxides under basic conditions leads to the related benzocarbaporphyrins **1a**−**c**.[8,14] The latter reaction is believed to be triggered by nucleophilic attack at position 2^3 on the azulene subunit. Three synthetic routes to azuliporphyrins have been developed. In the initial studies, azulene dicarbaldehyde **5** was reacted with tripyrrane **6** in TFA−CH_2Cl_2, followed by oxidation with DDQ or ferric chloride (Scheme 2) to give azuliporphyrins **4**.[7,8] Subsequently, tripyrrane analogue **7** was prepared by reacting azulene (**8**) with 2 equiv of an acetoxymethylpyrrole in refluxing acetic acid and isopropyl alcohol (Scheme 3).[8,15] Cleavage of the *tert*-butyl ester protective groups with TFA, condensation with a pyrrole dialdehyde **10**, and oxidation with DDQ or $FeCl_3$ gave good yields of azuliporphyrin **11**.[8,15] This route had the advantage of allowing the synthesis of heteroazuliporphyrins and a related dicarbaporphyrinoid system.[8,15] In the third route, *meso*-tetraarylazuliporphyrins **12** were shown to be accessible by reacting azulene, pyrrole, and an aromatic aldehyde in a 1:3:4 ratio in the presence of BF_3·Et_2O in chloroform, followed by oxidation with DDQ (Scheme 4).[16,17] Although *meso*-substituted azuliporphyrins **12**

SCHEME 1

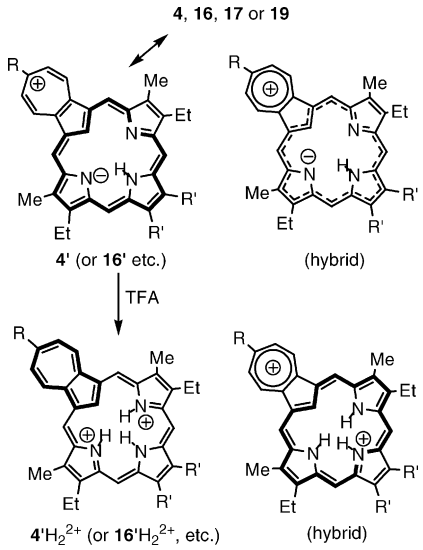

SCHEME 2

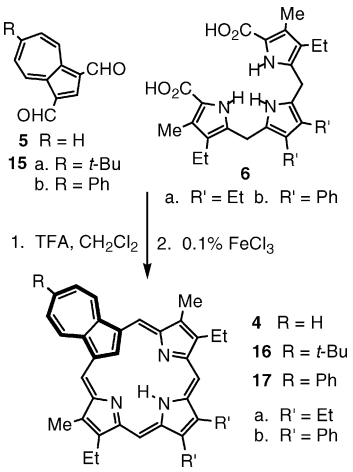

(3) Lash, T. D. In *The Porphyrin Handbook*; Kadish, K. M., Smith, K. M., Guilard, R., Eds.; Academic Press: San Diego, 2000; Vol. 2, pp 125−199.

(4) (a) Lash, T. D.; Hayes, M. J. *Angew. Chem., Int. Ed. Engl.* **1997**, *36*, 840−842. (b) Lash, T. D.; Hayes, M. J.; Spence, J. D.; Muckey, M. A.; Ferrence, G. M.; Szczepura, L. F. *J. Org. Chem.* **2002**, *67*, 4860−4874. (c) Liu, D.; Lash, T. D. *J. Org. Chem.* **2003**, *68*, 1755−1761.

(5) (a) Lash, T. D. *Angew. Chem., Int. Ed. Engl.* **1995**, *34*, 2533−2535. (b) Richter, D. T.; Lash, T. D. *Tetrahedron* **2001**, *57*, 3659−3673.

(6) (a) Lash, T. D.; Chaney, S. T. *Tetrahedron Lett.* **1996**, *37*, 8825−8828.

(7) Lash, T. D.; Chaney, S. T. *Angew. Chem., Int. Ed.* **1997**, *36*, 839−840. For an example of an azulisapphyrin, see: Richter, D. T.; Lash, T. D. *J. Org. Chem.* **2004**, *69*, 8842−8850.

(8) Lash, T. D.; Colby, D. A.; Graham, S. R.; Chaney, S. T. *J. Org. Chem.* **2004**, *69*, 8851−8864.

(9) Graham, S. R.; Ferrence, G. M.; Lash, T. D. *Chem. Commun.* **2002**, 894−895.

(10) Lash, T. D.; Colby, D. A.; Graham, S. R.; Ferrence, G. M.; Szczepura, L. F. *Inorg. Chem.* **2003**, *42*, 7326−7338.

(11) Srinivasan, A.; Furuta, H. *Acc. Chem. Res.* **2005**, *38*, 10−20.

(12) Harvey, J. D.; Ziegler, C. J. *Coord. Chem. Rev.* **2003**, *247*, 1−19.

(13) Colby, D. A.; Ferrence, G. M.; Lash, T. D. *Angew. Chem., Int. Ed.* **2004**, *43*, 1346−1349.

(14) Lash, T. D. *Chem. Commun.* **1998**, 1683−1684.

(15) Graham, S. R.; Colby, D. A.; Lash, T. D. *Angew. Chem., Int. Ed.* **2002**, *41*, 1371−1374.

(16) Colby, D. A.; Lash, T. D. *Chem. Eur. J.* **2002**, *8*, 5397−5402.

SCHEME 3

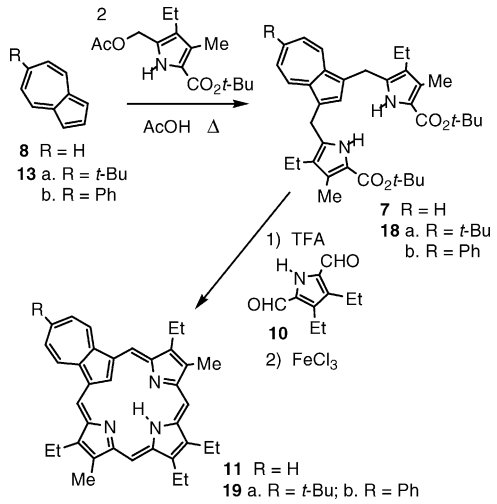

SCHEME 4

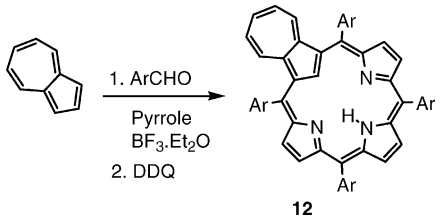

are reasonably soluble in solvents such as CH_2Cl_2 and $CHCl_3$, *meso*-unsubstituted azuliporphyrins **4** and **11** are only sparingly soluble in organic solvents, and this has made it difficult to obtain high-quality NMR data for the free base forms of these molecules.[8] The internal CH and NH proton resonances provide important data on the aromatic characteristics of carbaporphyrinoid systems, but these signals cannot be assigned with any degree of confidence for azuliporphyrins **4** or **11**.[8] In one case, the 21-CH resonance was tentatively identified in $CDCl_3$ solutions near 2 ppm,[8] but aggregation effects can also influence these chemical shifts and this makes the result difficult to fully interpret. Furthermore, it was not possible to obtain carbon-13 NMR data for the free base *meso*-unsubstituted azuliporphyrins.[8]

In order to further investigate the azuliporphyrin system, 2^3-*tert*-butyl- and 2^3-phenyl-substituted azuliporphyrins were targeted for synthesis. The presence of bulky substituents on the azulene ring was expected to inhibit aggregation effects[18] and thereby overcome the problems that had previously been encountered in obtaining high-quality NMR data. In addition, the synthesis of these azuliporphyrins was expected to be little affected by the presence of a substituent at this remote position on the azulene moiety. Substitution at position 2^3 also allows the macrocycle to retain a plane of symmetry, which simplifies spectroscopic characterization. In addition, compact units such as phenyl or *tert*-butyl groups sometimes aid in the isolation of X-ray quality crystals[4b,6b,9] and as no examples of free base azuliporphyrins have been structurally characterized previously this was an important consideration. Ring contraction reactions to give benzocarbaporphyrins are believed to involve initial nucleophilic attack at the 2^3-position[14] and substituted azuliporphyrins could also provide insightful information on the mechanism of this unusual reaction. All of these issues were addressed in the investigations of 2^3-substituted azuliporphyrins described below.[19]

SCHEME 5

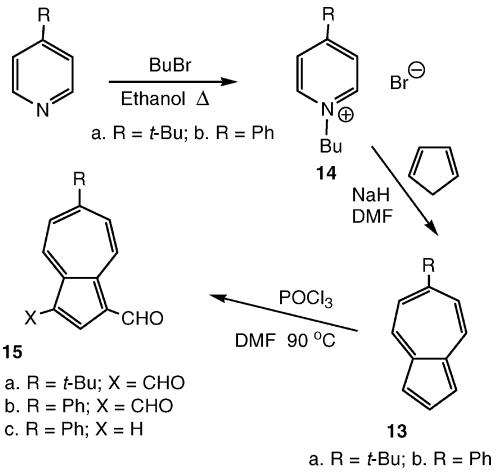

Results and Discussion

The key starting materials for these studies were 6-*tert*-butylazulene (**13a**) and 6-phenylazulene (**13b**). Although both of these compounds are known,[20,21] an alternative procedure was developed for the synthesis of these azulenes (Scheme 5).[22] Reaction of 4-*tert*-butyl or 4-phenylpyridine with 1-bromobutane in refluxing ethanol gave the corresponding pyridinium salts **14**. These reacted with cyclopentadiene and sodium hydride in DMF to afford the required azulenes **13**. Treatment of **13a** with phosphorus oxychloride and DMF at 90 °C gave the related dialdehyde **15a** (Scheme 5). Vilsmeier−Haack formylation of 6-phenylazulene (**13b**) was carried out similarly, although a mixture of dialdehyde **15b** and monaaldehyde **15c** were isolated in this case (Scheme 5). These were easily separated by column chromatography on silica.

The azulene dialdehydes **15a** and **15b** were reacted with tripyrranes **6a** or **6b** to give a series of four azuliporphyrins (**16a**,**b** and **17a**,**b**) in 55−67% yield (Scheme 2). The reaction was conducted using TFA−dichloromethane for the condensation and the final oxidation step involved shaking the reaction solution with 0.1% aqueous ferric chloride solution for 5 min.[23,24] Purification was easily accomplished by column chromatography on grade 3 basic alumina and further recrystallization from chloroform−hexanes. The alternative "3 + 1" route shown in Scheme 3 was also investigated.[15] As azulene favors electrophilic substitution at the 1 and 3 positions, it is possible to construct tripyrrane analogues by reacting **13** with 2 equiv of an acetoxymethylpyrrole **9** in the presence of a weak

(17) Lash, T. D.; Colby, D. A.; Ferrence, G. M. *Eur. J. Org. Chem.* **2003**, 4533−4548.

(18) Jiao, W.; Lash, T. D. *J. Org. Chem.* **2003**, *68*, 3896−3901.

(19) These results were presented, in part, at the following meeting: 229th National American Chemical Society Meeting, San Diego, California, March 2005 (El-Beck, J. A.; Lash, T. D. *Book of Abstracts*; American Chemical Society: Washington, DC, 2005; CHED 546).

(20) Ito, S.; Morita, N.; Asao, T. *Bull. Chem. Soc. Jpn.* **1995**, *68*, 1409−1436.

(21) Bergmann, E. D.; Ikan, R. *J. Am. Chem. Soc.* **1956**, *78*, 1482−1485.

(22) These procedues were adapted from a previously reported synthesis of 6-methylazulene: Rudolf, K.; Robinette, D.; Koenig, T. *J. Org. Chem.* **1987**, *52*, 641−647.

(23) Lash, T. D.; Richter, D. T.; Shiner, C. M. *J. Org. Chem.* **1999**, *64*, 7973−7982.

(24) Richter, D. T.; Lash, T. D. *Tetrahedron Lett.* **1999**, *40*, 6735−6738.

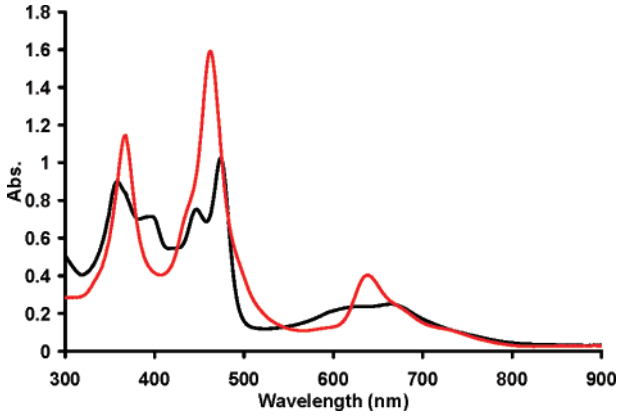

FIGURE 1. UV−vis spectra of azuliporphyrin **16a**. Black line: free base in 1% Et_3N−chloroform. Red line: dication **16a**H_2^{2+} in 1% TFA−chloroform.

acid catalyst. Azulene had been shown to react with **9** in refluxing AcOH−*i*-PrOH to give azulitripyrrane **7** in 59% yield. However, reactions of **13a** or **13b** with **9** were very solvent dependent, and poor results were obtained under the original conditions. The reactions were attempted in a number of different solvents, and the best yields of azulitripyrrane **18a** (55%) were obtained by reacting **13a** and **9** with acetic acid in ethyl acetate. However, these conditions did not work well for the phenyl-substituted version. The best results in this case were obtained when **13b** was reacted with **9** in refluxing acetic acid−ethanol, and following chromatography and recrystallization, azulitripyrrane **18b** was isolated in 49% yield. The tripyrrane analogues **18** were treated with TFA for 10 min, diluted with dichloromethane, and reacted with pyrrole dialdehyde **10**. Following oxidation with ferric chloride, column chromatrogaphy on grade 3 basic alumina, and recrystallization, azuliporphyrins **19a** and **19b** were obtained in 45−51% yield. Therefore, good results were obtained using 6-*tert*-butyl- and 6-phenylazulene in both of the "3 + 1" routes to azuliporphyrins. All of the azuliporphyrins obtained in these studies showed similar UV−vis spectra to the previously synthesized 2^3-unsubstituted azuliporphyrins **4** and **11**. For instance, azuliporphyrin **16a** in 1% Et_3N−$CHCl_3$ showed four medium absorption bands at 358, 397, 447, and 474 nm and a broad absorption centered on 665 nm (Figure 1). These spectra are very different from fully aromatic porphyrinoids such as **1** and **2** which show strong Soret bands and several smaller Q bands, and this reflects the unusual electronic features of the azuliporphyrin system. However, it is worth noting that the UV−vis spectra of the individual azuliporphyrins showed significant variations in the relative intensities and specific wavelengths for the absorption bands. In 1% TFA−$CHCl_3$, dications **16**H_2^{2+}, **17**H_2^{2+} or **19**H_2^{2+} were generated that showed that showed stronger Soret-like bands (Figure 1) that were consistent with increased porphyrin-type characteristics.

Five of the six new azuliporphyrins were sufficiently soluble in chloroform to give good proton and carbon-13 NMR data for the free base species. Triphenylazuliporphyrin **17b** gave poorly resolved proton NMR spectra in $CDCl_3$ due to aggregation, as had been the case for 2^3-unsubstituted azuliporphyrins **4** and **11**. The proton NMR spectrum for **16a** in $CDCl_3$ showed the *meso*-protons at two 2H singlets at 8.15 and 9.05 ppm, and the azulene protons appeared as two 2H doublets at 7.89 and 9.33 ppm (Figure 2). These shifts are consistent with a moderate diatropic ring current. The methyl substituents can also give

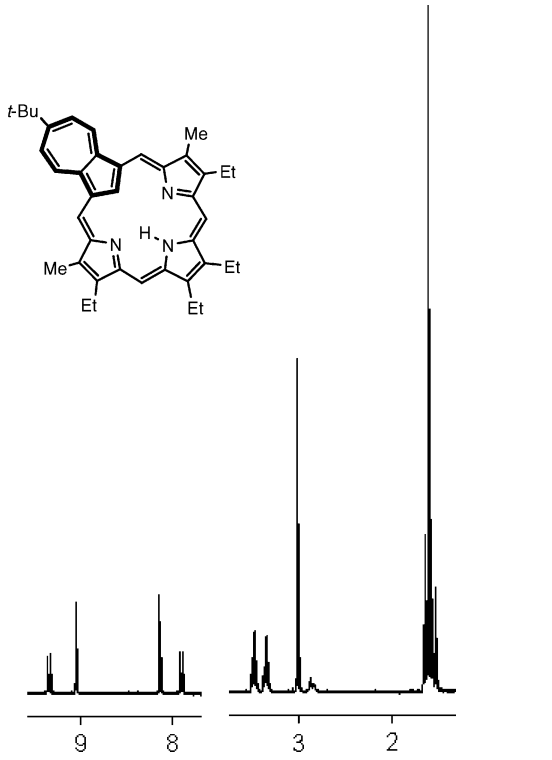

FIGURE 2. 400 MHz proton NMR spectrum of azuliporphyrin **16a** in $CDCl_3$.

some insights into the aromatic ring current. In a nonaromatic benziporphyrin,[25] these resonances are present at 2.4 ppm but in fully aromatic porphyrins the methyl resonances are typically near 3.6 ppm. In **16a**, the methyl resonance appears at an intermediary value of 3.02 ppm. Most importantly, two broad resonances were observed between 2.8 and 2.9 ppm integrating for a total of 2H (Figures 2 and 3). These correspond to the internal CH and NH protons, and significantly, the CH resonance shows up approximately 1 ppm downfield from the value tentatively assigned to azuliporphyrins **4**. The upfield shift for **4** is probable due to aggregation effects as none of the other spectroscopic features for **4** suggest that these azuliporphyrins are more diatropic than **16a**. When the NMR solution of **16a** was shaken with D_2O, a single sharper 1H peak remained at 2.82 ppm (Figure 3). Although deuterium exchange of the NH was expected, the CH undergoes an apparent upfield shift which we tentatively attribute to minor conformational changes due to hydrogen bonding interactions. The proton NMR spectrum for 2^3-phenylazuliporphyrin **17a** in $CDCl_3$ showed the internal protons as two broad 1H resonances at 3.23 and 3.30 ppm, and again these were replaced by a single slightly upfield shifted resonance following a D_2O shake. The downfield shift to the internal proton resonances indicates that the ring current for **17a** is less than for **16a**. The *meso*-proton resonances at 8.06 and 8.96 ppm and the azulene doublets at 7.81 and 9.29 ppm are also all slightly less deshielded for **17a** than the equivalent resonances for **16a** and even the methyl group resonance at 2.99 ppm is 0.03 ppm upfield from the value seen in **16a**. The opposite trends are seen for 12,13-diphenylazuliporphyrin **16b**. The internal CH and NH resonances were observed at 2.8 and 2.49 ppm, upfield from the values seen for **16a**, while the

(25) Lash, T .D.; Chaney, S. T.; Richter, D. T. *J. Org. Chem.* **1998**, *63*, 9076−9088.

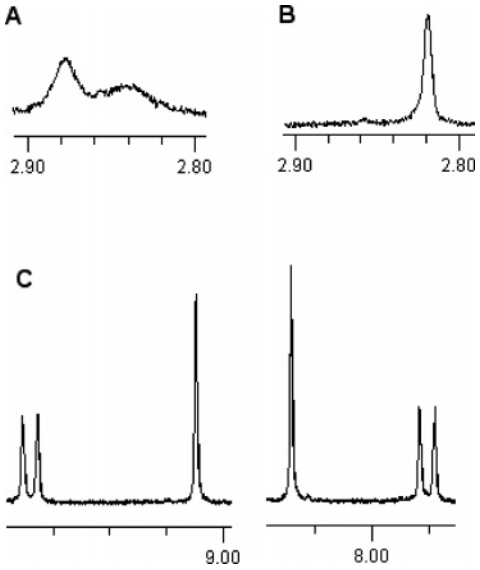

FIGURE 3. Details of the 400 MHz proton NMR spectrum of azuliporphyrin **16a** in $CDCl_3$. (A) Internal CH and NH resonances for free base azuliporphyrin **16a**. (B) The same region following a D_2O shake. In addition to the expected deuterium exchange for the NH, the CH sharpens and shifts slightly upfield. (C) Details of the downfield region.

peripheral protons were all further deshielded. The *meso*-protons gave two 2H resonances at 8.33 and 9.39 ppm, 0.18 and 0.34 ppm further downfield than the values for **16a**, and the azulene and methyl resonances also showed minor downfield shifts. The presence of an electron-donating *tert*-butyl substituent on the azulene ring helps stabilize the tropylium character in dipolar resonance contributors **16a′** (Scheme 1), and this helps to increase the contributions from these aromatic canonical forms. The decreased electron-donating ability of the phenyl substituents leads to the reduced diatropicity observed for **17a**. In **16a** and **17a**, the presence of electron-donating ethyl groups at the 12 and 13 positions would destabilize the carbaporphyrin anion character in the dipolar resonance contributors and the phenyl groups in this position for **16b** has a beneficial rather than detrimental effect. The data for **19a** and **19b** were similar to their isomers **16a** and **17a**, respectively. Azuliporphyrins **16**, **17a**, and **19** all gave carbon-13 NMR spectra in $CDCl_3$ that were consistent with proposed structures and showed the presence of a plane of symmetry. The *meso*-carbons gave rise to two resonances with chemical shift values of 93−96 ppm and 108−110 ppm.

Addition of one drop of TFA to NMR solutions of the azuliporphyrins gave the aromatic dications. The internal CH resonance for **16a**H_2^{2+} was observed at −3.19 ppm (Figure 4), while the values for **17a**, **16b**, and **17b** were −2.91, −3.43, and −2.69 ppm, respectively. The *meso*-protons were also significantly shifted downfield and **16a** shows two 2H resonances at 9.54 and 10.39 ppm (Figure 4). The values of these resonances in **17a**, **16b** and **17b** were 9.50 and 10.39, 9.66 and 10.50, and 9.47 and 10.36 ppm, respectively. These and other data from these spectra indicate that the diamagnetic ring currents for this series increased in the sequence **17b** < **17a** < **16b** < **16a**. The *tert*-butyl groups in **16a** and **16b** clearly still lead to an increased diatropicity compared to the related 2^3-phenyl substituted azuliporphyrins by stabilizing the tropylium ion character. However, the presence of phenyl groups at the 12,13-positions now leads to a decrease in the diamagnetic ring

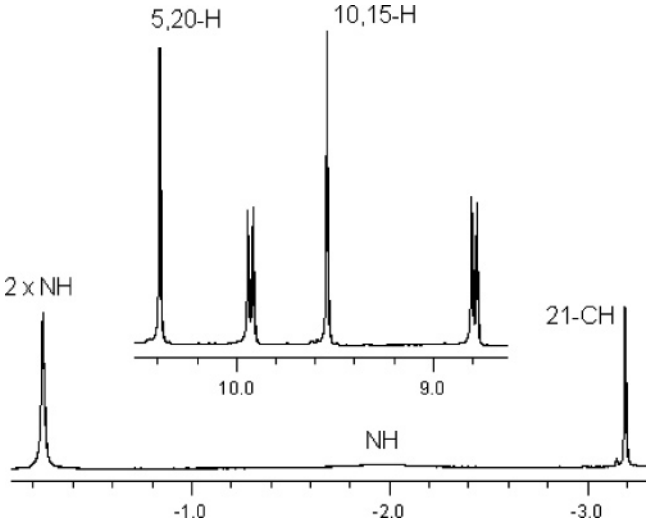

FIGURE 4. Partial 400 MHz proton NMR spectrum of azuliporphyrin dication **16a**H_2^{2+} in TFA−$CDCl_3$ showing the upfield and downfield regions.

current. This inversion in the trend seen for the free base azuliporphyrins is due to the electron-donating ethyl groups now stabilizing the protonated carbaporphyrinoid system. Again, the chemical shifts for **19a**H_2^{2+} and **19b**H_2^{2+} were similar to the isomeric species **16a**H_2^{2+} and **17a**H_2^{2+} and showed the same general trends. Carbon-13 NMR spectra for the protonated azuliporphyrins again showed the presence of a plane of symmetry. In addition, the *tert*-butylazuliporphyrins **16a**, **16b** and **19a** all showed a downfield resonance near 173 ppm due to the 2^3-carbon of the substituted tropylium species.

The proton NMR spectra of **16a** and **17a** were also examined in acetone-d_6, DMSO-d_6, and DMF-d_7. Although the internal protons did not resolve in most of these spectra, useful trends were noted for the external protons. For **16a**, the *meso*-protons were observed at 8.32 and 9.30, 8.33 and 9.48, and 8.42 and 9.47, for solutions in acetone-d_6, DMSO-d_6 and DMF-d_7, respectively. These downfield shifts are significantly increased compared to $CDCl_3$, particularly for the polar aprotic solvents DMSO and DMF, and similar downfield shifts were also noted for the azulene protons. Small downfield shifts were also observed for the methyl resonances and the same trends were observed for **17a**. These data imply that the diatropic character of these azuliporphyrins is solvent dependent, and the shifts are presumably due to stabilization of the dipolar resonance contributors by the more polar solvents. Proton NMR spectra were also obtained in pyridine-d_5, but these results were more difficult to interpret. For **16a**, the internal CH was noted at 3.36 ppm, and this downfield shift compared to spectra run in $CDCl_3$ implies a decreased ring current effect. However, the *meso*-protons were observed as two 2H singlets at 8.56 and 9.56 ppm, values that were 0.4−0.5 ppm further downfield than is seen for spectra in $CDCl_3$, and a downfield shift was also noted for one of the azulene doublets. Similar trends were seen for **17a**, **16b**, **17b**, **19a**, and **19b**. The anomalous value for the 21-CH may be due to small changes in the local environment or a minor conformation change due to hydrogen bonding interactions with the pyridine solvent. The remaining data suggest that pyridine increases the diatropic ring current in these azuliporphyrins, again by stabilizing the dipolar resonance contributors.

2^3-*tert*-Butylazuliporphyrin **16a** crystallized from dichloromethane−hexanes to give crystals that were suitable for X-ray

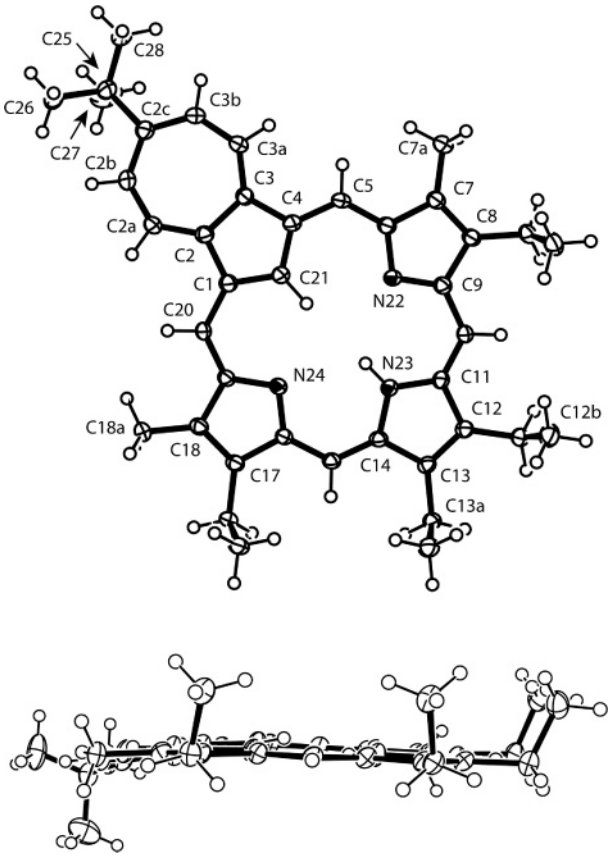

FIGURE 5. ORTEP-III drawing (50% probability level, hydrogen atoms drawn arbitrarily small) of compound **16a** viewed (a) normal to and (b) edge on with core N,N,N plane. Framework bond separations (Å): C(1)−C(2) 1.438(3), C(2)−C(2a) 1.391(3), C(2a)−C(2b) 1.390(3), C(2b)−C(2c) 1.410(3), C(2c)−C(3b) 1.402(3), C(3b)−C(3a) 1.391(3), C(3a)-C(3) 1.387(3), C(2)−C(3) 1.465(3), C(3)−C(4) 1.440(3), C(4)−C(21) 1.403(3), C(21)−C(1) 1.406(3), C(4)−C(5) 1.427(3), C(5)−C(6) 1.377(3), C(6)−C(7) 1.473(3), C(7)−C(8) 1.359(3), C(8)−C(9) 1.481(3), C(9)−C(10) 1.417(3), C(10)−C(11) 1.373(3), C(11)−C(12) 1.455(3), C(12)−C(13) 1.370(3), C(13)−C(14) 1.456(3), C(14)−C(15) 1.372(3), C(15)−C(16) 1.416(3), C(16)−C(17) 1.475(3), C(17)−C(18) 1.358(3), C(18)−C(19) 1.474(3), C(19)−C(20) 1.382(3), C(20)−C(1) 1.425(3), C(6)−N(22) 1.391(3), N(22)−C(9) 1.341(3), C(11)−N(23) 1.382(3), N(23)−C(14) 1.388(3), C(16)−N(24) 1.342(3), N(24)−C(19) 1.390(3).

diffraction analysis (Figure 5). This result was particularly significant because no structural data had previously been obtained for a free base azuliporphyrin. Difference Fourier maps clearly indicated the presence of electron density consistent with hydrogen atoms attached to the C(21) and N(23) atoms. The overall macrocycle is essentially planar as evidenced by the minimal 2.53(6)°, 1.09(6)°, and 1.65(5)° tilts between the pyrrole planes and the mean macrocyclic plane defined by the *meso*, pyrrolic, and C(1), C(2), C(3), and C(4) carbon atoms. The azulene as a whole displays a 7.40(3)° tilt out of the mean macrocyclic plane. This appears to be the result of both intermolecular packing forces and intramolecular steric crowding. The plane defined by atoms C(1), C(2), C(3), C(4), and C(21) displays a small 4.81(6)° tilt, easily ascribed to steric crowding in the central cavity due to the presence of two hydrogen atoms. The fully aromatic benzocarbaporphyrin **20a** and the related 21-chlorocarbaporphyrin **20b** (Chart 2) display respective 15.5° and 29.6° tilts of their indene units due to increasing steric crowding caused by the respective presence

CHART 2

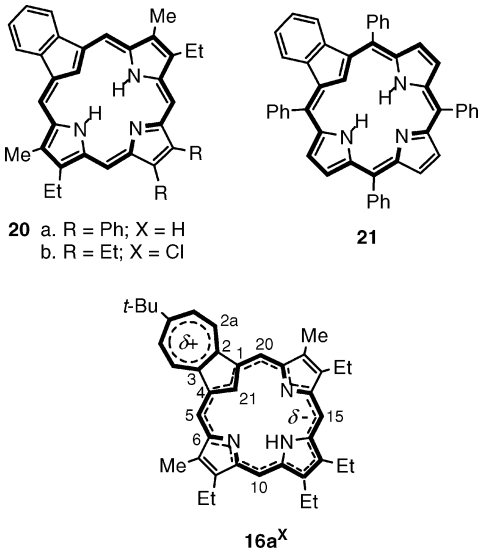

of three atoms in the central cavities.[4b,26] However, the related tetraphenylbenzocarbaporphyrin **21** exhibits an indene tilt of only 11.9° even though there are additional steric interactions with the *meso*-phenyl substituents.[17] Presumably packing forces are a significant factor affecting deformation from planarity. Nevertheless, the degree of planarity in these examples does not correlate with the degree of aromatic character observed in their proton NMR spectra. In **16a**, the plane defined by atoms C(2A), C(2B), C(2C), C(3B), and C(3A) has a 10.58(5)° tilt relative to the mean macrocyclic plane and a 5.80(7)° tilt relative to the plane defined by C(1), C(2), C(3), C(4), and C(21), which appears to be attributable to packing forces associated with contact between the azulene *tert*-butyl group and neighboring molecules. A Mogul geometry check of **16a** indicated bonding parameters to be normal with the exception of the C(2C)−C(25)−C(27) bond angle and the torsion angles associated with the *t*-Bu tertiary carbon atom.[27] At 105.9(2)°, the bond angle is more than 2σ more compressed than the 110.3 ± 1.9° average of parameters in a similar environment. This seems to be the result of packing forces between the hydrogen atoms attached to C(26) and C(28) and the neighboring molecule related by $2 - x$, $1 - y$, $1 - z$. By canting the *t*-Bu group away from the neighboring molecule, the closest intermolecular separations between the *t*-Bu group and C(21) and H(21) achieve van der Waals separation.

In common with benzocarbaporphyrins **20** and **21**, macrocycle **16a** shows bonds lengths consistent with a delocalized π-bond distribution. The aromatic pathway of the benzocarbaporphyrins are best depicted by the 18 atom pathway shown in bold, whereas the bond length data for **16a** suggests the presence of a markedly different pathway as shown for structure **16a^{X}** in Chart 2. Although the C−C bond lengths in the bold pathway fall into an approximate range of 1.37−1.45 Å, the C(6)−C(7), C(8)−C(9), C(16)−C(17), and C(18)−C(19) bonds are all greater than 1.47 Å, which are typical values for single-bond

(26) Lash, T. D.; Muckey, M. A.; Hayes, M. J.; Liu, D.; Spence, J. D.; Ferrence, G. M. *J. Org. Chem.* **2003**, *68*, 8558−8570.

(27) Bruno, I. J.; Cole, J. C.; Kessler, M.; Luo, J.; Motherwell, W. D. S.; Purkis, L. H.; Smith, B. R.; Taylor, R.; Cooper, R. I.; Harris, S. E.; Orpen, A. G. *J. Chem. Inf. Comput. Sci.* **2004**, *44*, 2133−2144. (b) Allen, F. H *Acta Crystallogr.* **2002**, *B58*, 380−388. (c) Cambridge Structural Database, version 5.28 (January 2007).

SCHEME 6

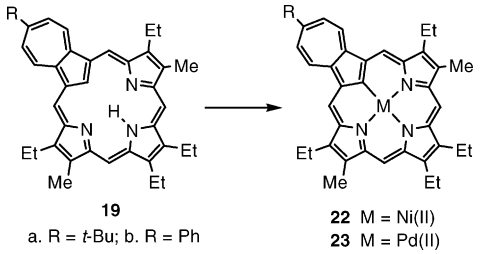

C(sp^2)−C(sp^2) interactions.[28] However, the C(7)−C(8) and C(17)−C(18) bond distances are the shortest C−C separations in the structure and are consistent with these atoms being isolated from the macrocycle's delocalized π-bond system. Although the C2−C3 distance is fairly long (1.465(3) Å), metalloazuliporphyrin structures also have a similarly long bond length at this location.[9,10] The middle pyrrole ring does show some bond length alternation, but this is much larger in the other two pyrrole units. It is worth noting that close examination of the framework metrics reveals sufficient variation in bond distances such that structural metrics alone are insufficient to determine the extent of π-delocalization in **16a**. Nevertheless, the data suggest that azuliporphyrins have significant aromatic character and the 17 atom delocalization pathway illustrated by structure **16a$^{\mathbf{X}}$** appears to be a significant contributor for this system.

The reactivity of 2^3-substituted azuliporphyrins was also investigated, but this work was restricted to studies on azuliporphyrins **19a** and **19b**. Azuliporphyrins have been shown to be excellent organometallic ligands,[9,10] and this property was investigated for the 2^3-substituted compounds (Scheme 6). The azuliporphyrins reacted with nickel(II) acetate in refluxing DMF to give the nickel(II) derivatives **22** in 86−97% yield. These derivatives were easily purified by column chromatography on grade 3 alumina. The *meso*-protons for **22a** appeared as two 2H singlets at 8.48 an 9.11 ppm, and these resonances appeared at virtually the same values in **22b**. These chemical shifts and other data from these spectra indicate that the two metal complexes have similar diatropic character. Azuliporphyrins **19a** and **19b** also reacted with palladium(II) acetate in refluxing DMF to give the palladium(II) complexes **23** in >80% yield. The *meso*-protons for **23a** gave two 2H singlets at 8.61 and 9.24 ppm, and again the phenyl-substituted metalloazuliporphyrin **23b** gave similar shifts. The palladium(II) complexes **23** appear to be slightly more diatropic than the nickel derivatives **22**, probably because Pd(II) is a better fit for the macrocyclic cavity which allows for a more planar structure.

Azuliporphyrins **4** undergo an unusual oxidative ring contraction reaction in the presence of peroxides under alkaline conditions to afford benzocarbaporphyrins **1a**−**c**. We have proposed[8,14] that this chemistry is triggered by a nucleophilic attack onto the azuliporphyrin macrocycle at position 2^3. The availability of 2^3-substituted azuliporphyrins such as **19a** and **19b** allowed us to further probe this interesting reaction. Azuliporphyrins were shown to reversibly form adducts with nucleophiles such as pyrrolidine to give species like **24** (Scheme 7). Although the pyrrolidine adduct was formed in equilibrium with azuliporphyrin **4**, addition of one drop of pyrrolidine to an NMR solution of **4** in $CDCl_3$ was sufficient to turn the green

SCHEME 7

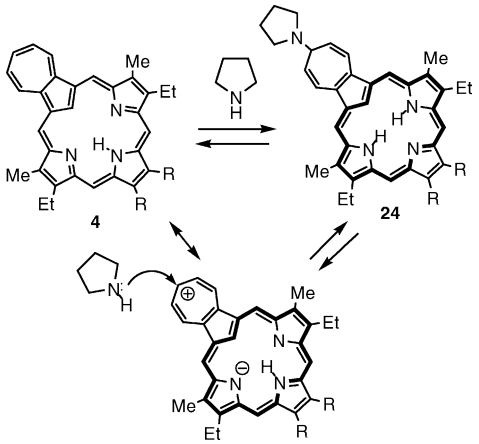

SCHEME 8

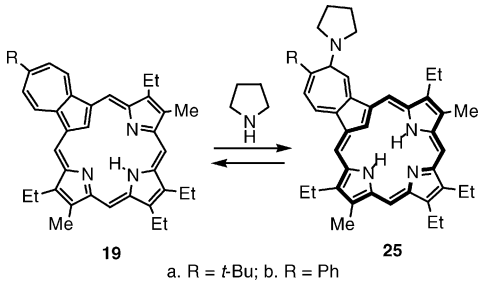

solution brown and to produce a proton NMR spectrum that was consistent with structure **24**.[8,14] Only one major species was present in the NMR spectrum, and a plane of symmetry was evident in part from the presence of only two 2H singlets for the *meso*-protons at 9.67 and 9.88 ppm.[8,14] The aromatic character of the adduct is greatly increased as can be seen from the values cited for the *meso*-proton resonances and the 21-CH resonance which was shifted upfield to −6.87 ppm. The methyl groups attached to the porphyrin macrocycle gave a 6H singlet at 3.53 ppm, providing further evidence of a powerful diatropic ring current in this species.[8,14] In order to see whether this type of adduct could still be formed for structures like **19a** and **19b**, proton NMR spectra for these azuliporphyrins were run in $CDCl_3$ in the presence of increasing concentrations of pyrrolidine-d_8. Addition of one drop of pyrrolidine to **19a** showed the presence of a new species, but the major peaks were due to the original azuliporphyrin (Figure 6A). This showed that the *tert*-butyl group shifts the equilibrium away from the formation of pyrrolidine adducts but does not prevent this chemistry from occurring. Addition of further amounts of d_8-pyrrolidine caused the equilibrium to further shift toward the formation of the pyrrolidine adduct and a single resonance was observed near −7 ppm for the 21-CH unit (Figure 6). The data are consistent with the formation of the asymmetrical adduct **25a** (Scheme 8) where the nucleophilic addition has taken place at the position adjacent to the *tert*-butyl moiety. Four 1H singlets were observed near 10 ppm for the *meso*-protons and the azulene protons were replaced by a series of four 1H doublets between 5.0 and 8.4 ppm. As the amount of pyrrolidine was increased, all of the resonances appeared to shift upfield by >0.3 ppm, but this was an artifact due to the residual chloroform peak being used as a reference (see the Supporting Information). When small volumes of pyrrolidine were added to an NMR tube containing $CDCl_3$ with a trace amount of TMS, the chloroform resonance was

(28) A Mogul search of C(sp^2, aromatic)−C(sp^2, nonaromatic) returned an average 1.48 ± 0.02 Å distance for over 500 hits.

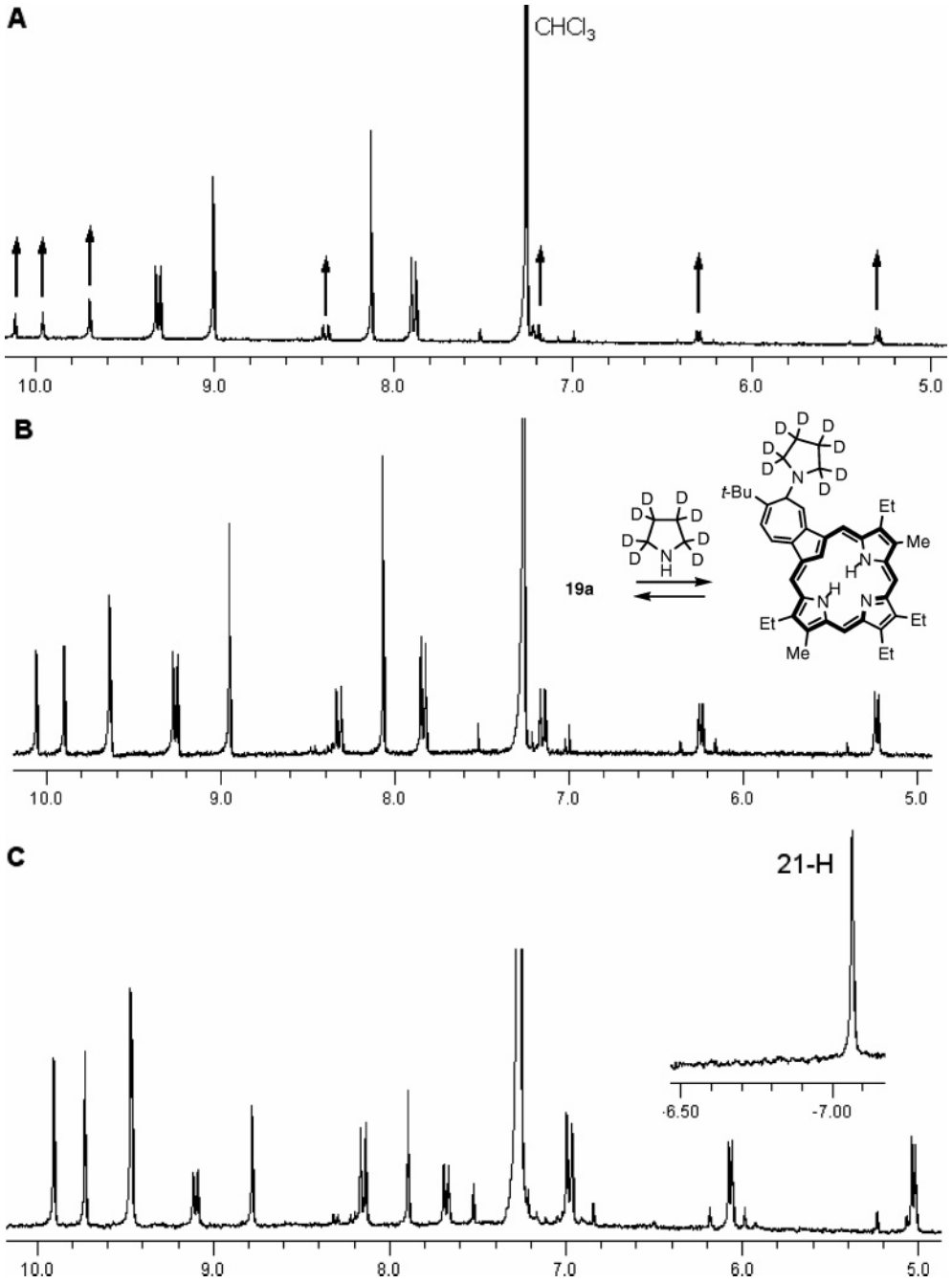

FIGURE 6. Partial 400 MHz proton NMR spectra of *tert*-butylazuliporphyrin **19a** in $CDCl_3$ with 1 drop (A), 4 drops (B), or 10 drops (C) of pyrrolidine-d_8. The peaks corresponding to pyrrolidine adduct **25a**, labeled with arrows in spectrum A, increase in relative intensity with increasing concentrations of pyrrolidine-d_8. The apparent upfield shift to the resonances is an artifact due to the residual chloroform signal shifting downfield due to interactions with the pyrrolidine. The inset upfield region shown for spectrum C shows the internal CH resonance of the aromatic adduct.

observed to shift downfield relative to the TMS standard in direct proportion to the amount of pyrrolidine added. This shift was attributed to a weak hydrogen bonding interaction between the chloroform and pyrrolidine and the data demonstrate that the use of solvent peaks as a reference can be unreliable. Therefore, the apparent shifts seen in Figure 6 are due to a downfield shift of the chloroform and not an upfield shift to the resonances for the pyrrolidine adduct. Proton NMR spectra for 2^3-phenylazuliporphyrin **19b** in the presence of pyrrolidine-d_8 gave similar results, although the presence of a second, albeit minor, species was evident. The major pyrrolidine adduct also lacked a plane of symmetry and the NMR data were consistent with the formation of species **25b**.

Initially, we had speculated that the presence of a *tert*-butyl group on the azulene ring would block oxidative ring contraction reactions to benzocarbaporphyrins. However, azuliporphyrins **19a** and **19b** both reacted rapidly with *t*-BuOOH and KOH at room temperature to give ring contraction products. The reactions were monitored by TLC, and these results indicated that the reactions were slightly faster for the substituted azuliporphyrins compared to reactions previously conducted for **4** under similar conditions. Treatment of these azuliporphyrins

SCHEME 9

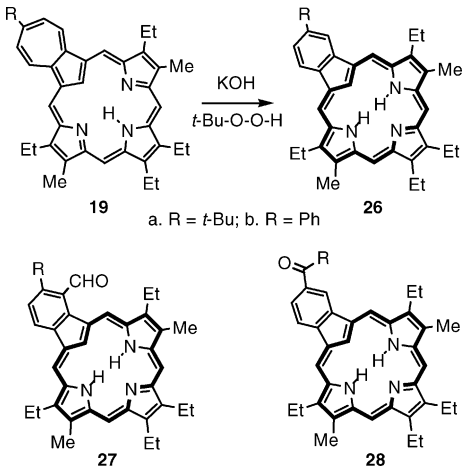

with 2.5 equiv of *t*-BuOOH in the presence of potassium hydroxide in methanol-dichloromethane gave two isolatable benzocarbaporphyrins, although 2^3-*tert*-butylazuliporphyrin **19a** gave one major product in 45% yield while **19b** gave roughly equal amounts of the two products in a combined yield of approximately 60%. The major carbaporphyrin product derived from **19a** showed the presence of a *tert*-butyl group and a 1,2,4-trisubstituted benzene moiety. On the basis of proton NMR and carbon-13 NMR spectroscopy and mass spectrometry, the product was identified as **26a** (Scheme 9). The less polar product from the reaction of **19b** with *t*-BuOOH and KOH were similarly characterized and shown to be the analogous phenyl-substituted benzocarbaporphyrin **26b**. The minor product from **19a** was only formed in trace amounts. The IR spectrum for this compound showed the presence of a carbonyl stretch at 1699 cm^{-1}, and HRMS gave a molecular formula of $C_{40}H_{45}N_3O$. Two plausible structures were considered for this minor product, the formyl derivative **27a** and ketone **28a**. The proton NMR spectrum showed two 1H doublets at 7.81 and 8.77 ppm (J = 8 Hz) and a series of five 1H singlets at 9.67, 9.69, 9.97, 10.03, and 11.86 ppm. If the product were the pivaloyl derivative **28a**, long-range coupling to the isolated benzene proton would be expected, but this is not seen in the NMR data. Also, the presence of a downfield resonance at 11.86 ppm is not consistent with structure **28a**, but the *meso*-proton adjacent to the formyl moiety in **27a** would be expected to give a strongly deshielded singlet in this region. As only trace amounts of this compound were formed, further spectroscopic analysis was not feasible. However, the more polar benzocarbaporphyrin derived from azuliporphyrin **19b** gave similar data and could be isolated in 27−42% yield. This product gave a carbonyl stretch in its IR spectrum at 1688 cm^{-1}, and the HRMS data gave a molecular formula of $C_{42}H_{41}N_3O$. The proton NMR data showed two 1H doublets for the benzo-unit at 7.77 and 9.00 ppm, and a series of five 1H singlets at 9.59, 9.65, 9.90, 10.62 and 11.38 ppm. These data were again a better fit for the aldehyde structure **27b** than for ketone **28b**, and the downfield singlet at 11.38 ppm could only be attributed to the close proximity of a carbonyl moiety to a *meso*-proton. Carbon-13 NMR spectroscopy gives a carbonyl resonance at 196.2 ppm and DEPT confirms that this corresponds to the CH of an aldehyde.

The structures of the carbaporphyrin products isolated from these reactions are consistent with the mechanisms shown in Scheme 10. Initial nucleophilic addition of a *tert*-butyl peroxide

SCHEME 10

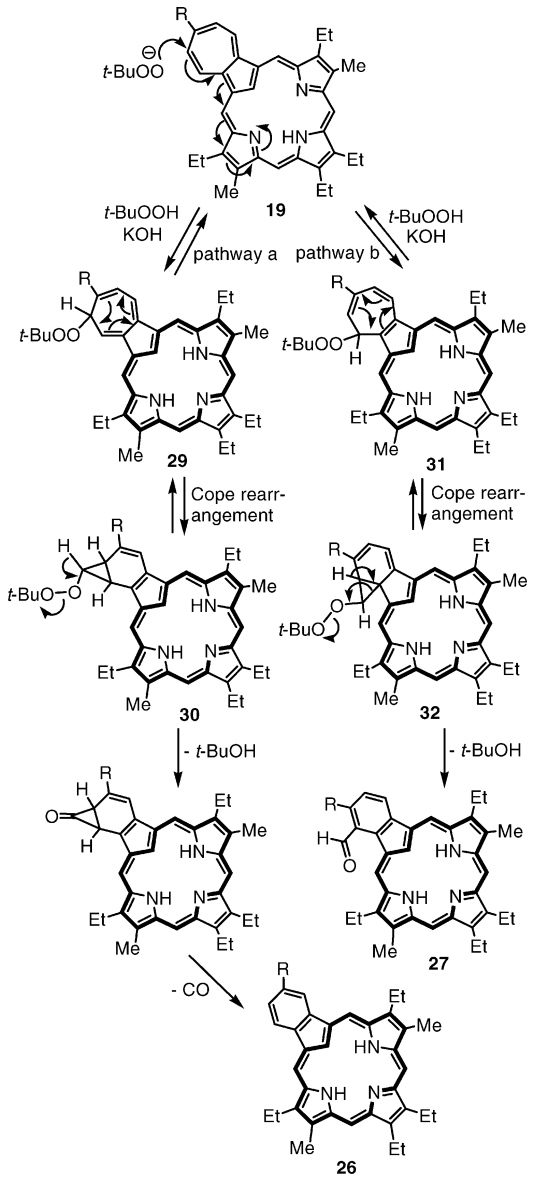

anion at position 2^2 on the azulene unit of **19** would give adduct **29** (pathway a) and subsequent Cope rearrangement would lead to the cyclopropane peroxide species **30**. Elimination of *tert*-butyl alcohol and extrusion of carbon monoxide would afford the substituted benzocarbaporphyrins **26**. Alternatively, addition at the sterically hindered 2^1-carbon would give adduct **31** (pathway b) and this could undergo a Cope rearrangement to give **32**. Subsequent elimination of *tert*-butyl alcohol would then afford the aldehydes **27**. Although the pyrrolidine experiments showed that the 2^2-adducts were strongly favored, particularly for **19a**, these additions are reversible and do not appear to control the regioselectivity for this chemistry. The formation of **27b** as a major product from the oxidative ring contraction of phenylazuliporphyrin **19b** is somewhat surprising, but if the elimination of *t*-BuOH is the rate-limiting step the *tert*-butyl group would sterically hinder pathway b. Certainly the steric bulk of the *tert*-butyl moiety in **19a** does effectively control the regioselectivity for this reaction compared to the 2^3-phenylazuliporphyrin **19b**.

Conclusion

A series of six azuliporphyrins were prepared from 6-*tert*-butyl and 6-phenylazulene using two different "3 + 1" strategies. These porphyrinoids were all formed in excellent yields and showed significant diatropic characteristics. The presence of a *tert*-butyl group on the azulene unit increased the diatropic properties of the azuliporphyrin macrocycle, and other substituent and solvent effects have been noted. One of the new azuliporphyrins gave crystals suitable for X-ray crystallographic analysis and the macrocycle was shown to be fairly planar and the bond lengths are consistent with the presence of a favored 17 atom delocalization pathway. Addition of pyrrolidine to NMR solutions of 2^3-substituted azuliporphyrins showed that the formation of nucleophilic adducts was sterically inhibited and the additions were primarily favored at the 2^2-position. However, although oxidative ring contractions of azuliporphyrins in the presence of *t*-BuOOH and KOH appear to involve an initial nucleophilic attack onto the azulene ring, the 2^3-substituents did not inhibit the formation of benzocarbaporphyrin products. Two different benzocarbaporphyrins were identified in these reactions, and the structures of these products provides insights into the mechanisms for these unusual oxidative ring contractions.

Experimental Section

1,3-Bis(5-*tert*-butoxycarbonyl-3-ethyl-4-methyl-2-pyrrolylmethyl)-6-*tert*-butylazulene (18a). 6-*tert*-Butylazulene (315 mg; 1.71 mmol) and *tert*-butyl 5-acetoxymethyl-4-ethyl-3-methylpyrrole-2-carboxylate (**9**)[30] (1.07 g; 3.80 mmol) were dissolved in ethyl acetate (25 mL) and acetic acid (5 mL). The mixture was flushed with nitrogen and stirred under reflux overnight. The solvent was evaporated to dryness on a rotary evaporator and the residue chromatographed on silica eluting initially with 20% hexanes−dichloromethane. A major deep blue band corresponding to the tripyrrane analogue was collected, the solvent evaporated, and the residue recrystallized from toluene to give **18a** (588 mg; 0.939 mmol; 55%) as blue crystals: mp 197−199 °C, with darkening at 170 °C; ^{1}H NMR ($CDCl_3$) δ 1.09 (6H, t, J = 7.6 Hz), 1.43 (9H, s), 1.47 (18H, s), 2.26 (6H, s), 2.50 (4H, q, J = 7.5 Hz), 4.28 (4H, s), 7.25 (2H, d, partially obscured by chloroform peak), 7.41 (1H, s), 8.10 (2H, br), 8.12 (2H, d, J = 10.4 Hz); ^{13}C NMR ($CDCl_3$): δ 10.7, 15.7, 17.6, 24.3, 28.8, 32.1, 38.8, 80.1, 118.8, 120.6, 123.4, 124.3, 126.1, 131.8, 132.8, 135.9, 137.8, 161.5, 162.2; HRMS (EI) calcd for $C_{40}H_{54}N_2O_4$ *m*/*z* 626.4084, found 626.4083. Anal. Calcd for $C_{40}H_{54}N_2O_4$: C, 76.64; H, 8.68; N, 4.47. Found: C, 76.37; H, 8.80; N, 4.50.

1,3-Bis(5-*tert*-butoxycarbonyl-3-ethyl-4-methyl-2-pyrrolylmethyl)-6-phenylazulene (18b). 6-Phenylazulene (350 mg; 1.71 mmol) and acetoxymethylpyrrole **9**[30] (1.07 g; 3.80 mmol) in acetic acid (5 mL) and ethanol (25 mL) were reacted under the previous conditions. Recrystallization from toluene gave the tripyrrane analogue (539 mg; 0.834 mmol; 49%) as blue crystals, mp 177−180 °C, with darkening at 170 °C: ^{1}H NMR ($CDCl_3$) δ 1.09 (6H, t, J = 7.6 Hz), 1.48 (18H, s), 2.26 (6H, s), 2.50 (4H, q, J = 7.5 Hz), 4.32 (4H, s), 7.29 (2H, d, J = 10.4 Hz), 7.39−7.44 (1H, m), 7.45−7.50 (2H, m), 7.47 (1H, s), 7.61−7.64 (2H, m), 8.16 (2H, br s), 8.22 (2H, d, J = 10.4 Hz); ^{13}C NMR ($CDCl_3$) δ 10.7, 15.7, 17.6, 24.4, 28.8, 80.2, 118.9, 123.0, 123.6, 125.4, 126.1, 128.3, 128.7, 128.9, 131.5, 133.0, 136.0, 138.6, 145.4, 152.2, 161.6; HRMS (EI) calcd for $C_{42}H_{50}N_2O_4$ *m*/*z* 646.3771, found 646.3765. Anal. Calcd for $C_{42}H_{50}N_2O_4$: C, 77.98; H, 7.79; N, 4.33. Found: C, 77.80; H, 7.68; N, 4.41.

2^3-*tert*-Butyl-8,12,13,17-tetraethyl-7,18-dimethylazuliporphyrin (16a). Tripyrranedicarboxylic acid **6a**[31,32] (100 mg; 0.221 mmol) was stirred with TFA (1 mL) under nitrogen for 2 min. The solution was diluted with dichloromethane (19 mL), 6-*tert*-butyl-1,3-azulenedicarbaldehyde (53 mg; 0.221 mmol) was added, and the resulting mixture was stirred overnight in the dark. The solution was diluted with chloroform and shaken vigorously with 0.1% aqueous ferric chloride solution (200 mL) for 5 min. The organic layer was separated and the aqueous solution back-extracted with chloroform. The combined organic solutions were washed with water and then with 5% aqueous sodium bicarbonate, and the organic phase was evaporated under reduced pressure. The residue was loaded onto a grade 3 basic alumina column and eluted initially with dichloromethane and then with chloroform. A deep green fraction was collected and evaporated under reduced pressure and the residue recrystallized from chloroform−hexanes to give the *tert*-butylazuliporphyrin (71 mg; 0.125 mmol; 57%) as purple crystals: mp >300 °C; UV−vis (1% Et_3N−$CHCl_3$) λ_{max} (log ϵ) 358 (4.81), 397 (4.71), 447 (4.74), 474 (4.81), 618 (sh, 4.23), 665 nm (4.26); UV−vis (1% TFA−$CHCl_3$) λ_{max} (log ϵ) 368 (4.92), 462 (5.06), 638 nm (4.46); ^{1}H NMR ($CDCl_3$) δ 1.58 (6H, t, J = 7.6 Hz), 1.60 (9H, s), 1.64 (6H, t, J = 7.8 Hz), 2.84 (1H, v br), 2.88 (1H, br), 3.02 (6H, s), 3.37 (4H, q, J = 7.6 Hz), 3.50 (4H, q, J = 7.6 Hz), 7.89 (2H, d, J = 10.8 Hz), 8.15 (2H, s), 9.05 (2H, s), 9.33 (2H, d, J = 11.2 Hz); ^{1}H NMR (TFA−$CDCl_3$) δ −3.19 (1H, s), −2.0 (1H, v br), −0.25 (2H, br s), 1.65 (6H, t, J = 7.8 Hz), 1.72 (9H, s), 1.75 (6H, t, J = 7.6 Hz), 3.47 (6H, s), 3.81−3.91 (8H, 2 overlapping quartets), 8.79 (2H, d, J = 11.2 Hz), 9.54 (2H, s), 9.93 (2H, d, J = 10.8 Hz), 10.39 (2H, s); ^{1}H NMR (pyridine-d_5): δ 1.49 (9H, s), 1.57−1.64 (12H, 2 overlapping triplets), 3.11 (6H, s), 3.36 (1H, s), 3.42−3.50 (8H, 2 overlapping quartets), 7.88 (2H, d, J = 11.2 Hz), 8.56 (2H, s), 9.53 (2H, d, J = 10.8 Hz), 9.56 (2H, s); ^{1}H NMR (acetone-d_6) δ 1.57 (6H, t, J = 7.6 Hz), 1.66 (9H, s), 1.68 (6H, t, J = 8 Hz), 2.62 (1H, v br), 2.77 (1H, br), 3.05 (6H, s), 3.42 (4H, q, J = 7.6 Hz), 3.60 (4H, q, J = 7.6 Hz), 8.18 (2H, d, J = 10.4 Hz), 8.32 (2H, s), 9.30 (2H, s), 9.69 (2H, d, J = 10.4 Hz); ^{1}H NMR (DMF-d_7) δ 1.57 (6H, t, J = 7.6 Hz), 1.65 (9H, s), 1.67 (6H, t, J = 7.2 Hz), 3.10 (6H, s), 3.45 (4H, q, obscured by water peak), 3.63 (4H, q, J = 7.6 Hz), 8.23 (2H, d, J = 10.8 Hz), 8.42 (2H, s), 9.47 (2H, s), 9.88 (2H, d, J = 10.8 Hz); ^{1}H NMR (DMSO-d_6) δ 1.53 (6H, t, J = 7.6 Hz), 1.60 (9H, s), 1.62 (6H, t, J = 7.2 Hz), 3.05 (6H, s), 3.39 (4H, q, J = 7.6 Hz), 3.57 (4H, q, J = 7.6 Hz), 8.21 (2H, d, J = 10.8 Hz), 8.33 (2H, s), 9.38 (2H, s), 9.82 (2H, d, J = 11.2 Hz); ^{13}C NMR ($CDCl_3$) δ 11.1, 16.6, 19.1, 19.4, 31.9, 39.0, 93.3, 108.0, 126.6, 130.1, 134.2, 136.3, 139.5, 139.8, 141.9, 142.7, 148.1, 155.2, 161.6, 164.4; ^{13}C NMR (TFA−$CDCl_3$) δ 11.6, 16.1, 17.0, 19.7, 19.8, 31.7, 40.6, 95.1, 110.0, 124.1, 128.6, 139.3, 140.9, 141.6, 141.9, 142.1, 143.8, 144.5, 146.6, 153.1, 158.6, 173.3; HRMS (EI) calcd for $C_{40}H_{45}N_3$ + 2H *m*/*z* 569.3770, found 569.3780. Anal. Calcd for $C_{40}H_{45}N_3 \cdot {}^1/_5CHCl_3$: C, 81.60; H, 7.70; N, 7.10. Found: C, 81.56; H, 7.81; N, 7.08.

8,12,13,17-Tetraethyl-7,18-dimethyl-2^3-phenylazuliporphyrin (17a). Using the same conditions, tripyrrane **6a** (100 mg 0.221 mmol) was reacted with dialdehyde **15b** (57.5 mg; 0.221 mmol). Recrystallization from chloroform-hexanes gave the phenylazuliporphyrin (80.5 mg; 0.137 mmol; 62%) as dark purple crystals, mp >300 °C; UV−vis (1% Et_3N−$CHCl_3$): λ_{max} (logϵ) 361 (4.77), 399 (4.73), 447 (4.77), 475 (4.89), 628 nm (4.30); UV−vis (1% TFA-$CHCl_3$): λ_{max} (logϵ) 380 (4.80), 466 (5.07), 642 nm (4.49); ^{1}H NMR ($CDCl_3$): δ 1.56 (6H, t, J = 7.6 Hz), 1.62 (6H, t, J = 7.6 Hz), 2.99 (6H, s), 3.23 (1H, v br), 3.30 (1H, s) 3.33 (4H, q, J = 7.6 Hz), 3.46 (4H, q, J = 7.7 Hz), 7.52−7.56 (1H, m), 7.57−7.61 (2H, m), 7.76 (2H, d, J = 8 Hz), 7.81 (2H, d, J = 9.6 Hz), 8.06

(29) Ito, S.; Morita, N.; Asao, T. *Bull. Chem. Soc. Jpn.* **1999**, *72*, 2543−2548.

(30) Clezy, P. S.; Crowley, R. J.; Hai, T. T. *Aust. J. Chem.* **1982**, *35*, 411−421.

(31) Sessler, J. L.; Johnson, M. R.; Lynch, V. *J. Org. Chem.* **1987**, *52*, 4394−4397.

(32) Lash, T. D. *J. Porphyrins Phthalocyanines* **1997**, *1*, 29−44.

(2H, s), 8.96 (2H, s), 9.29 (2H, d, J = 10 Hz); ^{1}H NMR (TFA−$CDCl_3$) δ −2.91 (1H, s), −1.79 (1H, v br), −0.11 (2H, br s), 1.66 (6H, t, J = 7.8 Hz), 1.75 (6H, t, J = 7.6 Hz), 3.47 (6H, s), 3.81−3.90 (8H, 2 overlapping quartets), 7.69−7.75 (3H, m), 7.89−7.92 (2H, m), 8.77 (2H, d, J = 10.4 Hz), 9.50 (2H, s), 9.97 (2H, d, J = 11.2 Hz), 10.39 (2H, s); ^{1}H NMR (pyridine-d_5) δ 1.56−1.62 (12H, 2 overlapping triplets), 3.02 (6H, s), 3.38−3.46 (8H, 2 overlapping quartets), 3.7 (1H, v br), 3.78 (1H, s), 7.5−7.6 (3H, m, obscured by solvent), 7.85−7.87 (2H, m), 7.95 (2H, d, J = 10.4 Hz), 8.47 (2H, s), 9.52 (2H, s), 9.70 (2H, d, J = 10.8 Hz); ^{1}H NMR (acetone-d_6) δ 1.56 (6H, t, J = 7.6 Hz), 1.66 (6H, t, J = 7.4 Hz), 3.03 (6H, s), 3.39 (4H, q, J = 7.6 Hz), 3.56 (4H, q, J = 7.4 Hz), 7.59−7.63 (1H, m), 7.68 (2H, t, J = 7.4 Hz), 7.96 (2H, d, J = 7.2 Hz), 8.12 (2H, d, J = 10.4 Hz), 8.24 (2H, br s), 9.26 (2H, s), 9.74 (2H, d, J = 10.8 Hz); ^{1}H NMR (DMF-d_7) δ 1.57 (6H, t, J = 7.4 Hz), 1.66 (6H, t, J = 7.6 Hz), 2.80 (1H, s), 3.08 (6H, s), 3.42 (4H, q, obscured by water peak), 3.60 (4H, q, J = 7.6 Hz), 7.61−7.65 (1H, m), 7.67−7.72 (2H, m), 8.02−8.05 (2H, m), 8.20 (2H, d, J = 10.8 Hz), 8.34 (2H, s), 9.45 (2H, s), 9.96 (2H, d, J = 10.4 Hz); ^{1}H NMR (DMSO-d_6) δ 1.52 (6H, t, J = 7.6 Hz), 1.60 (6H, t, J = 7.6 Hz), 3.04 (6H, s), 3.37 (4H, q, J = 7.6 Hz), 3.54 (4H, q, J = 7.5 Hz), 7.59−7.63 (1H, m), 7.66−7.70 (2H, m), 7.97 (2H, d, J = 7.2 Hz), 8.17 (2H, d, J = 10.8 Hz), 8.25 (2H, s), 9.36 (2H, s), 9.87 (2H, d, J = 11.2 Hz); ^{13}C NMR ($CDCl_3$) δ 11.1, 16.6, 17.1, 19.1, 19.3, 93.4, 108.1, 126.9, 128.3, 129.0, 129.3, 131.9, 134.2, 136.9, 139.6, 139.9, 142.0, 143.1, 144.0, 147.4, 153.7, 155.5, 162.1; ^{13}C NMR (TFA−$CDCl_3$) δ 11.6, 16.0, 16.9, 19.7, 19.8, 95.1, 110.1, 123.6, 128.7, 129.0, 130.2, 131.4, 139.4, 141.4, 141.9, 142.1, 142.3, 144.1, 144.9, 147.1, 152.4; HRMS (EI) calcd for $C_{42}H_{41}N_3$ + 2H m/z 589.3457, found 589.3454. Anal. Calcd for $C_{40}H_{45}N_3 \cdot {}^1/_4CHCl_3$: C, 82.16; H, 6.73; N, 6.80. Found: C, 82.05; H, 6.70; N, 6.85.

2^3-*tert*-Butyl-8,17-diethyl-7,18-dimethyl-12,13-diphenylazuliporphyrin (16b). Tripyrrane **6b**[4b] (100 mg; 0.182 mmol) was reacted with 6-*tert*-butyl-1,3-azulenedicarbaldehyde (44 mg; 0.183 mmol) under the foregoing conditions. The crude product was chromatographed on grade 3 basic alumina, eluting with chloroform, and recrystallized from chloroform−hexanes to afford the porphyrin analogue (66 mg; 0.10 mmol; 55%) as purple crystals: mp >300 °C; UV−vis (1% Et_3N−$CHCl_3$) λ_{max} (log ϵ) 371 (4.79), 405 (4.74), 433 (4.77), 477 (4.79), 557 (4.06), 677 nm (4.24); UV−vis (1% TFA−$CHCl_3$) λ_{max} (log ϵ) 374 (4.81), 466 (4.97), 644 nm (4.42); ^{1}H NMR ($CDCl_3$) δ 1.50 (6H, t, J = 7.6 Hz), 1.62 (9H, s), 2.49 (1H, br s), 2.8 (1H, v br), 3.04 (6H, s), 3.25 (4H, q, J = 7.6 Hz), 7.49−7.59 (6H, m), 7.77 (4H, d, J = 8 Hz), 7.95 (2H, d, J = 10.4 Hz), 8.33 (2H, s), 9.17 (2H, s), 9.39 (2H, d, J = 10.4 Hz); ^{1}H NMR (TFA−$CDCl_3$) δ −3.43 (1H, s), −1.8 (1H, v br), −0.53 (2H, br s), 1.58 (6H, t, J = 7.8 Hz), 1.73 (9H, s), 3.49 (6H, s), 3.74 (4H, q, J = 7.6 Hz), 7.68−7.74 (6H, m), 7.82−7.85 (4H, m), 8.85 (2H, d, J = 10.8 Hz), 9.66 (2H, s), 9.98 (2H, d, J = 10.4 Hz), 10.5 (2H, s, obscured by TFA); ^{1}H NMR (pyridine-d_5) δ 1.50 (9H, s), 1.52 (6H, t, J = 7.2 Hz), 2.90 (1H, br s), 3.14 (6H, s), 3.30 (4H, q, J = 7.6 Hz), 7.50 (2H, t, J = 7.4 Hz), 7.60 (4H, t, J = 7.4 Hz), 7.92−7.98 (6H, m), 8.79 (2H, s), 9.63 (2H, d, J = 10.8 Hz), 9.72 (2H, s); ^{13}C NMR ($CDCl_3$) δ 11.2, 16.5, 19.3, 31.9, 39.1, 96.5, 108.1, 126.8, 127.8, 128.5, 130.9, 132,1, 134.5, 134.9, 135.8, 139.3, 139.5, 141.9, 142.4, 148.8, 155.4, 161.5, 164.7; ^{13}C NMR (TFA−$CDCl_3$) δ 11.5, 15.8, 19.6, 31.6, 40.6, 98.4, 109.6, 123.7, 129.0, 129.4, 129.6, 132.0,139.4, 141.4, 142.2, 142.4, 142.7, 146.3, 153.4, 173.6; HRMS (EI) calcd for $C_{48}H_{45}N_3$ + 2H m/z 655.3770; found: 655.3771. Anal. Calcd for $C_{48}H_{45}N_3 \cdot 0.3CHCl_3$: C, 82.91; H, 6.52; N, 6.01. Found: C, 82.88; H, 6.46; N, 6.25.

8,17-Diethyl-7,18-dimethyl-2^3,12,13-triphenylazuliporphyrin (17b). Tripyrrane **6b**[4b] (100 mg; 0.182 mmol) was reacted with 6-phenyl-1,3-azulenedicarbaldehyde (47 mg; 0.181 mmol) under the foregoing conditions. The crude product was chromatographed on grade 3 basic alumina, eluting with chloroform, and recrystallized from chloroform−hexanes to afford the porphyrin analogue (83 mg; 0.12 mmol; 67%) as a dark green powder: mp >300 °C; UV−vis (1% Et_3N−$CHCl_3$) λ_{max} (log ϵ) 373 (4.85), 405 (4.79), 451 (4.82), 479 (4.93), 646 nm (4.37); UV−vis (1% TFA−$CHCl_3$) λ_{max} (log ϵ) 387 (4.85), 471 (5.09), 650 nm (4.56); ^{1}H NMR ($CDCl_3$) δ 1.47 (6H, t, J = 7.8 Hz), 3.03 (6H, br s), 3.17−3.28 (4H, br q), 7.50−7.63 (9H, m), 7.73 (4H, d, J = 7 Hz), 7.78 (2H, d, J = 7 Hz), 7.89 (2H, br), 8.24 (2H, br), 9.08 (2H, br), 9.35 (2H, br); ^{1}H NMR (TFA−$CDCl_3$) δ −2.69 (1H, s), 0.7 (2H, v br), 1.57 (6H, t, J = 7.6 Hz), 3.44 (6H, s), 3.67 (4H, q, J = 7.6 Hz), 7.65−7.71 (9H, m), 7.80−7.83 (4H, m), 7.86−7.90 (2H, m), 8.69 (2H, d, J = 10.4 Hz), 9.47 (2H, s), 9.93 (2H, d, J = 10.8 Hz), 10.36 (2H, s); ^{1}H NMR (pyridine-d_5) δ 1.50 (6H, t, J = 7.6 Hz), 3.05 (6H, s), 3.25 (4H, q, J = 7.6 Hz), 3.35 (1H, br s), 3.5 (1H, v br), 7.47−7.61 (9H, m), 7.87−7.93 (6H, m), 8.02 (2H, d, J = 10.8 Hz), 8.68 (2H, s), 9.68 (2H, s), 9.79 (2H, d, J = 10.4 Hz); ^{13}C NMR (TFA−$CDCl_3$) δ 11.5, 15.9, 19.6, 98.6, 109.5, 123.7, 128.7, 128.9, 129.2, 129.3, 130.0, 131.1, 132.0, 132.6,139.1, 141.0, 141.4, 141.9, 142.1, 142.5, 145.1, 146.8, 152.2, 160.3; HRMS (EI) calcd for $C_{50}H_{41}N_3$ + 2H m/z 685.3457, found 685.3457. Anal. Calcd for $C_{50}H_{41}N_3 \cdot {}^1/_8CHCl_3$: C, 86.15; H, 5.93; N, 6.01. Found: C, 85.87; H, 5.81; N, 6.23.

2^3-*tert*-Butyl-7,12,13,18-tetraethyl-8,17-dimethylazuliporphyrin (19a). Azulitripyrrane analogue **18a** (220 mg; 0.35 mmol) was stirred in TFA (6 mL) under nitrogen for 10 min. The reaction mixture was diluted with dichloromethane (200 mL), 3,4-diethylpyrrole-2,5-dicarbaldehyde[32,33] (63 mg; 0.35 mmol) was added, and the reaction mixture was stirred overnight in the dark. The solution was shaken vigorously in a separatory funnel with 0.1% aqueous ferric chloride solution (300 mL) for 5 min. The organic layer was separated and the aqueous solution back-extracted with chloroform. The combined organic solutions were washed with water and then with 5% aqueous sodium bicarbonate, and the organic phase was dried over sodium sulfate and evaporated under reduced pressure. The residue was purified on a grade 3 basic alumina column, eluting with chloroform, and the product was collected as a deep green fraction that followed a brown prefraction. The solvent was removed on a rotary evaporator and the residue recrystallized from chloroform−hexanes to give the *tert*-butylazuliporphyrin (102.3 mg; 0.18 mmol; 51%) as dark purple crystals: mp >300 °C; UV−vis (1% Et_3N−$CHCl_3$) λ_{max} (log ϵ) 357 (4.78), 400 (sh), 446 (4.64), 474 (4.75), 663 nm (4.15); UV−vis (1% TFA−$CHCl_3$) λ_{max} (log ϵ) 365 (4.81), 460 (5.00), 634 (4.41), 728 nm (3.83); UV−vis (1% pyrrolidine−$CHCl_3$) λ_{max} (log ϵ) 368 (4.65), 402 (4.68), 445 (4.57), 473 (4.59), 619 nm (4.01); UV−vis (5% pyrrolidine−$CHCl_3$) λ_{max} (log ϵ) 368 (4.62), 402 (4.62), 449 (4.59), 581 nm (4.11); UV−vis (10% pyrrolidine−$CHCl_3$) λ_{max} (log ϵ) 397 (4.58), 451 (4.60), 586 nm (4.11); ^{1}H NMR ($CDCl_3$) δ 1.61 (9H, s), 1.58−1.65 (12H, 2 overlapping triplets), 2.8 (1H, v br), 2.86 (1H, br), 2.92 (6H, s), 3.43−3.52 (2 overlapping quartets), 7.92 (2H, d, J = 10.8 Hz), 8.16 (2H, s), 9.04 (2H, s), 9.35 (2H, d, J = 10.8 Hz); ^{1}H NMR (TFA−$CDCl_3$) δ −3.33 (1H, s), −2.30 (1H, br), −0.60 (2H, s), 1.65 (9H, s), 1.61−1.70 (12H, 2 overlapping triplets), 3.31 (6H, s), 3.81 (4H, q, J = 7.8 Hz), 3.87 (4H, q, J = 7.8 Hz), 8.75 (2H, d, J = 10.4 Hz), 9.51 (2H, s), 9.88 (2H, d, J = 10.4 Hz), 10.32 (2H, s); ^{1}H NMR (pyridine-d_5) δ 1.49 (9H, s), 1.61 (6H, t, J = 7.6 Hz), 1.67 (6H, t, J = 7.6 Hz), 2.98 (6H, s), 3.27 (1H, v br), 3.35 (1H, s), 3.49 (4H, q, J = 7.6 Hz), 3.59 (4H, q, J = 7.5 Hz), 7.87 (2H, d, J = 10.4 Hz), 8.58 (2H, s), 9.57 (2H, d, J = 10 Hz), 9.58 (2H, s); ^{1}H NMR (10 drops of pyrrolidine-d_8−$CDCl_3$; peaks for 2^2-pyrrolidine adduct **25a** only) δ −7.06 (1H, s), −4.5 (2H, v br), 1.13 (9H, s,), 2.18−2.23 (12H, 2 overlapping triplets), 3.35 (6H, obscured by solvent impurities), 3.68 (4H, q, J = 7.6 Hz), 3.82 (4H, q, J = 7.6 Hz), 5.03 (1H, d, J = 7.6 Hz), 6.07 (1H, d, J = 8 Hz), 6.98 (1H, d, J = 12 Hz), 8.15 (1H, d, J = 12 Hz), 9.46 (1H, s), 9.47 (1H, s), 9.73 (1H, s), 9.91 (1H, s); ^{13}C NMR ($CDCl_3$) δ 11.0, 17.1, 17.3, 19.1, 19.5, 31.9, 39.0, 93.2, 107.9, 126.6, 130.2, 134.2, 134.8, 136.2, 139.9, 142.8,

(33) Tardieux, C.; Bolze, F.; Gros, C. P.; Guilard, R. *Synthesis* **1998**, 267−268.

146.6, 148.1, 154.1, 162.3, 164.4; ^{13}C NMR (TFA−$CDCl_3$) δ 11.2, 16.2, 16.9, 19.8, 20.1, 31.5, 40.8, 95.4, 109.3, 122.8, 128.7, 136.1, 139.6, 141.0, 141.5, 143.8, 145.4, 147.3, 148.8, 153.2, 173.5; HR MS (EI) calcd for $C_{40}H_{45}N_3$ + 2H *m*/*z* 569.3770, found 569.3771. Anal. Calcd for $C_{40}H_{45}N_3 \cdot {}^1/_{20}CHCl_3$: C, 83.83; H, 7.91; N, 7.32. Found: C, 83.52; H, 7.93; N, 7.32.

7,12,13,18-Tetraethyl-8,17-dimethyl-2^3-phenylazuliporphyrin (19b). Using the same procedure, tripyrrane analogue **18b** (228 mg; 0.353 mmol) gave the phenylazuliporphyrin (93.2 mg; 0.159 mmol; 45%) as dark green crystals: mp >300 °C (chloroform−hexanes); UV−vis (1% Et_3N−$CHCl_3$) λ_{max} (log ϵ) 358 (4.85), 398 (4.76), 447 (4.78), 475 (4.89), 628 nm (4.31); UV−vis (1% TFA−$CHCl_3$) λ_{max} (log ϵ) 354 (4.77), 380 (4.76), 464 (5.14), 638 (4.53); UV−vis (1% pyrrolidine−$CHCl_3$) λ_{max} (log ϵ) 368 (4.76), 403 (4.82), 445 (4.77), 474 (4.78), 526 (4.05), 567 (4.10), 624 nm (4.19); UV−vis (5% pyrrolidine−$CHCl_3$) λ_{max} (log ϵ) 407 (4.84), 472 (4.76), 525 (4.14), 564 (4.15), 616 nm (4.10); UV−vis (10% pyrrolidine−$CHCl_3$) λ_{max} (log ϵ) 403 (4.79), 451 (4.81), 536 (4.17), 585 nm (4.31); ^{1}H NMR ($CDCl_3$) δ 1.58−1.65 (12H, 2 overlapping triplets), 2.90 (6H, s), 3.15 (1H, v br), 3.30 (1H, v br) 3.42−3.49 (8H, 2 overlapping quartets), 7.51−7.62 (3H, m), 7.78−7.81 (2H, m), 7.86 (2H, d, J = 10.8 Hz), 8.07 (2H, s), 8.97 (2H, s), 9.33 (2H, d, J = 10 Hz); ^{1}H NMR (TFA−$CDCl_3$) δ −3.06 (1H, s), −2.17 (1H, v br), −0.54 (2H, br s), 1.69−1.77 (12H, 2 overlapping triplets), 3.38 (6H, s), 3.89 (4H, q, J = 7.6 Hz), 3.96 (4H, q, J = 7.6 Hz), 7.72−7.75 (3H, m), 7.89−7.92 (2H, m), 8.81 (2H, d, J = 10.4 Hz), 9.57 (2H, s), 10.00 (2H, d, J = 10.8 Hz), 10.42 (2H, s); ^{1}H NMR (pyridine-d_5) δ 1.57−1.63 (12H, 2 overlapping triplets), 2.93 (6H, s), 3.42−3.54 (8H, 2 overlapping quartets), 3.65 (1H, v br), 3.78 (1H, br s), 7.5−7.6 (3H, m, obscured by solvent), 7.85−7.88 (2H, m), 7.94 (2H, d, J = 10.4 Hz), 8.48 (2H, s), 9.55 (2H, s), 9.75 (2H, d, J = 10.8 Hz); ^{1}H NMR (10 drops of pyrrolidine-d_8−$CDCl_3$; partial data for major pyrrolidine adduct **25b**) δ −6.91 (1H, s), −4.0 (2H, v br), 5.33 (1H, d, J = 8 Hz), 6.41 (1H, d, J = 8 Hz), 7.2−7.4 (4H, m), 7.50 (2H, d, J = 7 Hz), 8.43 (1H, d, J = 11.6 Hz), 9.55 (2H, s), 9.86 (1H, s), 10.00 (1H, s); ^{13}C NMR ($CDCl_3$) δ 10.9, 17.1 (2), 19.0, 19.4, 93.3, 107.6, 126.8, 128.3, 129.1, 129.3, 132.2, 134.4, 134.6, 140.2, 143.8, 146.6, 147.4, 153.9; ^{13}C NMR (TFA−$CDCl_3$) δ 11.1, 16.2, 16.8, 19.6, 20.0, 95.3, 109.5, 123.0, 128.5, 128.9, 130.2, 131.5, 135.9, 139.3, 140.9, 141.2, 142.3, 144.0, 145.1, 147.7, 148.7, 152.2; HRMS (ESI) calcd for $C_{42}H_{41}N_3$ + H *m*/*z* 588.3379, found 588.3378. Anal. Calcd for $C_{42}H_{41}N_3 \cdot {}^1/_{10}CHCl_3$: C, 84.31; H, 6.91; N, 7.01. Found: C, 84.39; H, 7.01; N, 7.09.

[2^3-*tert*-Butyl-7,12,13,18-tetraethyl-8,17-dimethylazuliporphyrinato]nickel(II) (22a). A solution of *tert*-butylazuliporphyrin **19a** (7.7 mg, 0.0136 mmol) and nickel(II) acetate tetrahydrate (10 mg) in DMF (10 mL) was heated with stirring under reflux for 20 min. The solution was cooled to room temperature, diluted with chloroform, washed with water, and dried over sodium sulfate. The solvent was evaporated under aspirator pressure, and residual DMF was removed using an oil pump. The residue was purified by column chromatography on grade 3 alumina eluting with 20% hexanes−dichloromethane. Recrystallization from chloroform−methanol gave the nickel(II) derivative (8.2 mg, 0.0132 mmol, 97%) as dark purple crystals: mp >300 °C; UV−vis ($CHCl_3$) λ_{max} (log ϵ) 386 (4.70), 457 (4.52), 550 nm (4.36); ^{1}H NMR ($CDCl_3$) δ 1.46 (9H, s), 1.53−1.59 (12H, 2 overlapping triplets), 2.95 (6H, s), 3.40 (4H, q, J = 7.7 Hz), 3.48 (4H, q, J = 7.5 Hz), 7.68 (2H, d, J = 10.8 Hz), 8.48 (2H, s), 8.93 (2H, d, J = 10.4 Hz), 9.11 (2H, s); ^{13}C NMR ($CDCl_3$) δ 11.2, 17.2, 17.4, 19.2, 19.6, 31.7, 38.8, 95.7, 106.4, 128.7, 129.4, 132.7, 134.1, 143.5, 144.4, 144.7, 148.6, 151.5, 152.3, 155.6, 161.3; HRMS (EI) calcd for $C_{40}H_{43}N_3Ni$ *m*/*z* 623.2810, found 623.2812.

[7,12,13,18-Tetraethyl-8,17-dimethyl-2^3-phenylazuliporphyrinato]nickel(II) (22b). Using the foregoing conditions, phenylazuliporphyrin **19b** (10.0 mg; 0.0170 mmol) reacted with nickel(II) acetate tetrahydrate (10 mg) in DMF (10 mL) to afford the nickel(II) derivative **22b** (9.4 mg; 0.0146 mmol; 86%) as dark purple crystals: mp >300 °C (chloroform−methanol); UV−vis ($CHCl_3$) λ_{max} (log ϵ) 388 (4.82), 461 (4.64), 560 nm (4.56); ^{1}H NMR ($CDCl_3$) δ 1.59−1.65 (12H, 2 overlapping triplets), 3.00 (6H, s), 3.45 (4H, q, J = 7.6 Hz), 3.53 (4H, q, J = 7.7 Hz), 7.50−7.59 (3H, m), 7.66 (2H, d, J = 10.8 Hz), 7.74 (2H, d, J = 7 Hz), 8.49 (2H, s), 8.95 (2H, d, J = 10.8 Hz), 9.11 (2H, s); ^{13}C NMR ($CDCl_3$) δ 11.2, 17.1, 17.4, 19.2, 19.5, 95.7, 106.5, 127.8, 128.7, 128.9, 129.2, 129.3, 134.3, 134.6, 143.6, 144.2, 144.7, 144.9, 149.0, 159.7, 152.8, 157.3; HRMS (EI) calcd for $C_{42}H_{39}N_3Ni$ *m*/*z* 643.2497, found 643.2493.

[2^3-*tert*-Butyl-7,12,13,18-tetraethyl-8,17-dimethylazuliporphyrinato]palladium(II) (23a). Azuliporphyrin **19a** (10.0 mg; 0.0176 mmol) and palladium(II) acetate (10.0 mg) were reacted under the same conditions. Following chromatography on grade 3 alumina, eluting with 20% hexanes−dichloromethane, and recrystallization from chloroform−methanol, the palladium(II) complex (9.6 mg; 0.0143 mmol; 81%) was isolated as dark purple crystals: mp >300 °C; UV−vis ($CHCl_3$) λ_{max} (log ϵ) 366 (4.82), 416 (4.73), 448 (4.71), 568 nm (4.43); ^{1}H NMR ($CDCl_3$) δ 1.46 (9H, s), 1.61 (12H, t, J = 7.6 Hz), 3.03 (6H, s), 3.46 (4H, q, J = 7.6 Hz), 3.57 (4H, q, J = 7.7 Hz), 7.75 (2H, d, J = 10.8 Hz), 8.61 (2H, s), 9.04 (2H, d, J = 10.8 Hz), 9.24 (2H, s); ^{13}C NMR ($CDCl_3$) δ 11.3, 17.3, 17.5, 19.2, 19.5, 31.6, 38.8, 96.4, 108.4, 125.4, 130.1, 133.3, 133.5, 142.0, 142.8, 143.3, 147.4, 149.7, 152.8, 161.6; HRMS (EI) calcd for $C_{40}H_{43}N_3Pd$ *m*/*z* 671.2492, found 671.2487.

[7,12,13,18-tetraethyl-8,17-dimethyl-2^3-phenylazuliporphyrinato]palladium(II) (23b). Phenylazuliporphyrin **19b** (10.0 mg; 0.017 mmol) reacted with palladium(II) acetate (10.0 mg) under the same conditions to give the palladium(II) derivative (9.7 mg; 0.014 mmol; 82%) as dark purple crystals: mp >300 °C (chloroform−methanol); UV−vis ($CHCl_3$) λ_{max} (log ϵ) 368 (4.58), 422 (4.79), 449 (4.82), 583 nm (4.51); ^{1}H NMR ($CDCl_3$) δ 1.68 (12H, t, J = 7.6 Hz), 3.08 (6H, s), 3.50 (4H, q, J = 7.6 Hz), 3.61 (4H, q, J = 7.6 Hz), 7.51−7.61 (3H, m), 7.72−7.77 (4H, 2 overlapping doublets), 8.62 (2H, s), 9.06 (2H, d, J = 10.4 Hz), 9.24 (2H, s); ^{13}C NMR ($CDCl_3$; 50 °C) δ 11.3, 17.2, 17.4, 19.3, 19.6, 96.5, 108.6, 125.7, 127.9, 128.8, 129.3, 129.9, 133.6, 135.2, 142.6, 143.1, 143.7, 144.2, 148.1, 150.4, 151.1, 152.2; HRMS (EI) calcd for $C_{42}H_{39}N_3Pd$ *m*/*z* 691.2179, found 691.2183.

Oxidative Ring Contraction of 2^3-*tert*-Butyl-7,12,13,18-tetraethyl-8,17-dimethylazuliporphyrin. Potassium hydroxide (240 mg) in methanol (30 mL) was added to a solution of *tert*-butylazuliporphyrin **19a** (23 mg; 0.040 mmol) in dichloromethane (30 mL) and the resulting stirred mixture was purged with nitrogen for 10 min. A solution of *tert*-butyl hydroperoxide in decane (5 M, 20 μL) was added and the resulting solution stirred under nitrogen in the dark at room temperature for 2 h. The solution was diluted with chloroform, washed with water (2×), dried over sodium sulfate, and evaporated under reduced pressure. The residues were chromatographed on a grade 3 alumina column, eluting initially with hexanes and then with 50% dichloromethane−hexanes. The major orange band was collected, the solvent evaporated, and the residue recrystallized from chloroform−hexanes to give red-brown crystals (9.8−10.0 mg; 0.0176−0.0180 mmol; 44−45%) corresponding to *tert*-butylbenzocarbaporphyrin **26a**. A second minor band was collected (0.8−1.9 mg; 0.0014−0.0032 mmol; 3.5−8%) corresponding to the related aldehyde **27a**.

2^2-*tert*-Butyl-7,12,13,18-tetraethyl-8,17-dimethylbenzo[*b*]carbaporphyrin (26a): mp 289 °C with decomposition at 265 °C; UV−vis (1% Et_3N−$CHCl_3$) λ_{max} (logϵ) 379 (4.78), 427 (5.20), 511 (4.37), 545 (4.28), 604 (3.87), 664 nm (3.58); ^{1}H NMR ($CDCl_3$) δ −6.69 (1H, s), −3.92 (2H, br), 1.84−1.91 (12H, 2 overlapping triplets), 3.60 (3H, s), 3.61 (3H, s), 3.97 (4H, q, J = 7.6 Hz), 4.08−4.18 (4H, 2 overlapping quartets), 7.81 (1H, dd, J = 1.4, 7.8 Hz), 8.76 (1H, d, J = 8 Hz), 8.87 (1H, d, J = 1.6 Hz), 9.80 (1H, s), 9.81 (1H, s), 10.09 (1H, s), 10.13 (1H, s); ^{13}C NMR ($CDCl_3$) δ 11.2, 17.5, 18.6, 19.9, 20.1, 32.2, 35.5, 95.5, 98.3, 98.5, 109.9,

117.5, 120.2, 123.9, 130.6, 134.2, 134.5, 134.7, 136.3, 139.3, 139.4, 141.5, 144.3, 150.0, 152.7; HRMS (EI) calcd for $C_{39}H_{45}N_3$ *m*/*z* 555.3613, found 555.3617.

2^2-*tert*-Butyl-7,12,13,18-tetraethyl-2^1-formyl-8,17-dimethylbenzo[*b*]carbaporphyrin (27a): IR $\nu_{C=O}$ 1699 cm^{-1}; UV−vis (1% Et_3N−$CHCl_3$) λ_{max} (log ϵ) 377 (4.64), 426 (5.20), 511 (4.24), 547 (4.23), 604 (3.83); ^{1}H NMR ($CDCl_3$) δ −6.97 (1H, s), 1.76−1.82 (12H, m), 3.50 (3H, s), 3.52 (3H, s), 3.87 (4H, q, J = 7.6 Hz), 3.96−4.05 (4H, m), 7.81 (1H, d, J = 8 Hz), 8.77 (1H, d, J = 8 Hz), 9.67 (1H, s), 9.69 (1H, s), 9.97 (1H, s), 10.03 (1H, s), 11.86 (1H, s); HRMS (EI) calcd for $C_{40}H_{45}N_3O$ *m*/*z* 583.3563, found 583.3568.

Oxidative Ring Contraction of 7,12,13,18-Tetraethyl-8,17-dimethyl-2^3-phenylazuliporphyrin. Phenylazuliporphyrin **19b** (24.0 mg; 0.041 mmol) was reacted with *tert*-butyl hydroperoxide (5 M in hexane, 20 μL) in the presence of potassium hydroxide using the procedure described above. The crude product was run through a grade 3 alumina column, eluting with 50% dichloromethane−hexanes, and two major orange-brown bands were collected. The first band was evaporated down and the residue recrystallized from chloroform−methanol to give phenylbenzocarbaporphyrin **26b** (6.2−9.1 mg; 0.011−0.016 mmol; 27−39%) as a red-brown solid, mp 289 °C with decomposition at 283 °C. The more polar band was also evaporated down and recrystallized from chloroform−methanol to give the carbaporphyrin aldehyde **27b** (6.9−10.6 mg; 0.011−0.017 mmol; 27−42%) as red-brown crystals, mp 291 °C with decomposition at 287 °C.

7,12,13,18-Tetraethyl-8,17-dimethyl-2^2-phenylbenzo[*b*]carbaporphyrin (26b): UV−vis (1% Et_3N−$CHCl_3$) λ_{max} (log ϵ) 383 (4.76), 430 (5.19), 512 (4.32), 547 (4.35), 604 (3.84), 665 nm (3.46); ^{1}H NMR ($CDCl_3$) δ −6.67 (1H, s), −4.0 (2H, v br), 1.85−1.89 (12H, 2 overlapping triplets), 3.61 (6H, s), 3.97 (4H, q, J = 7.7 Hz), 4.09−4.16 (4H, 2 overlapping quartets), 7.49 (1H, t, J = 7.4 Hz), 7.64 (2H, t, J = 7.8 Hz), 7.81 (1H, dd, J = 1.6, 7.6 Hz), 8.03−8.06 (2H, m), 8.89 (1H, d, J = 8 Hz), 9.04 (1H, d, J = 1.6 Hz), 9.80 (2H, s), 10.12 (1H, s), 10.16 (1H, s); ^{13}C NMR ($CDCl_3$) δ 11.2, 17.5, 18.6, 20.0, 20.1, 95.6, 98.5, 98.6, 110.1, 119.6, 120.8, 125.8, 127.3, 127.8, 129.1, 130.6, 133.6, 133.7, 134.7, 136.5, 139.6 (2), 140.0, 140.7, 142.2, 142.9, 144.4, 153.0; HR MS (EI) calcd for $C_{41}H_{41}N_3$ *m*/*z* 575.3300, found 575.3293.

7,12,13,18-Tetraethyl-2^1-formyl-8,17-dimethyl-2^2-phenylbenzo[*b*]carbaporphyrin (27b): IR: $\nu_{C=O}$ 1688 cm^{-1}; UV−vis (1% Et_3N−$CHCl_3$) λ_{max} (log ϵ) 358 (4.74), 376 (4.75), 429 (5.27), 488 (4.15), 514 (4.31), 552 (4.41), 605 (3.94), 667 nm (3.54); ^{1}H NMR ($CDCl_3$) δ −7.01 (1H, s), −4.15 (2H, v br), 1.80−1.85 (9H, m), 1.90 (3H, t, J = 7.4 Hz), 3.52 (3H, s), 3.55 (3H, s), 3.89 (4H, q, J = 7.8 Hz), 4.03 (2H, q, J = 7.7 Hz), 4.12 (2H, q, J = 7.7 Hz), 7.53−7.57 (1H, m), 7.60−7.64 (2H, m), 7.71−7.74 (2H, m), 7.77 (1H, d, J = 7.6 Hz), 9.00 (1H, d, J = 7.6 Hz), 9.59 (1H, s), 9.65 (1H, s), 9.90 (1H, s), 10.62 (1H, s), 11.38 (1H, s); ^{1}H NMR (trace acid−$CDCl_3$; monocation) δ −6.51 (1H, s), −3.3 (1H, v br), −1.94 (1H, br s), −1.78 (1H, br s), 1.73 (3H, t, J = 7.8 Hz), 1.78 (3H, t, J = 7.6 Hz), 1.87 (6H, t, J = 7.4 Hz), 3.54 (3H, s), 3.56 (3H, s), 4.03−4.13 (8H, m), 7.52−7.57 (1H, m), 7.61 (2H, t, J = 7.2 Hz), 7.71 (2H, d, J = 7.2 Hz), 7.78 (1H, d, J = 7.6 Hz), 8.97 (1H, d, J = 7.6 Hz), 9.99 (1H, s), 10.01 (1H, s), 10.36 (1H, s), 10.50 (1H, s), 11.74 (1H, s); ^{13}C NMR ($CDCl_3$) δ 11.2, 17.4, 17.5, 18.6, 20.0, 20.1, 20.2, 94.7, 95.6, 98.1, 105.4, 111.2, 124.1, 128.1, 128.6, 128.7, 130.0, 130.1, 130.6, 130.9, 131.8, 132.6, 134.0, 134.2, 137.5, 138.6, 140.2, 140.8, 142.0, 142.7, 144.4, 144.7, 145.5, 153.3, 153.8, 196.2; HRMS (EI) calcd for $C_{42}H_{41}N_3O$ *m*/*z* 603.3250, found 603.3253.

Crystallographic Experimental Details of 16a. X-ray quality crystals were obtained by layering hexane onto a dichloromethane solution of **16a** and allowing the solvents to gradually diffuse into one another. The crystals were suspended in mineral oil at ambient temperature and a suitable crystal was selected. A mineral oil coated dark green plate thereby obtained of approximate dimensions 0.48 × 0.12 × 0.04 mm was mounted on a 50 mm MicroMesh MiTeGen Micromount and transferred to a Bruker AXS SMART APEX CCD diffractometer. The X-ray diffraction data were collected at −173 °C using Mo−K_a (λ = 0.71073 Å) radiation. Data collection and cell refinement were performed using SMART and SAINT+, respectively.[34] The unit cell parameters were obtained from a least-squares refinement of 6582 centered reflections. Compound **16a** was found to crystallize in the triclinic crystal system with the following unit cell parameters: a = 10.2118(8) Å, b = 12.0005(10) Å, c = 13.2831(11) Å, α = 87.9668(15)°, β = 74.7962(15)°, γ = 88.7667(16)°, Z = 2. The crystal system and lack of systematic absences indicated the space group to be *P*1 (no. 1) or *P*-1 (no. 2).[35] The latter was chosen on the basis that E-statistics strongly suggested a centrosymmetric structure and a sensible, quality refinement was obtained. A total of 16847 reflections were collected, of which 7749 were unique, and 4342 were observed $F_o^2 > 2_\sigma(F_o^2)$. Limiting indicies were as follows: $-13 \le h \le 13$, $-15 \le k \le 15$, $-17 \le l \le 17$. Data reduction were accomplished using SAINT.[34b] The data were corrected for absorption using the SADABS procedure.[34c]

Solution and data analysis were performed using the WinGX software package.[36] The structure of **16a** was solved by direct methods using the program SIR2004[37] and the refinement was completed using the program SHELX-97.[38] All non-hydrogen atoms were refined anisotropically. The H atoms attached to atoms C21 and N23 were identified through difference Fourier synthesis and refined with isotropic displacement parameters. All other H atoms were included in the refinement in the riding-model approximation (C−H Ar, CH_3, CH_2 = 0.95, 0.98 Å and 0.99 Å), with isotropic displacement parameters fixed at Ar, CH_2 = 1.2Ueq and CH_3 = 1.5Ueq of the parent atom. Atoms C7A and C18A were refined as idealized disordered methyl groups with H atoms included using the HFIX 123 instruction in SHELXL97. Full-matrix least-squares refinement on F^2 led to convergence, $(\Delta/\sigma)_{max}$ = 0.000, $(\Delta/\sigma)_{mean}$ = 0.0000, with R_1 = 0.0640 and wR_2 = 0.1509 for 7749 data with $F_o^2 > 2s(F_o^2)$ using 0 restraints and 396 parameters. A final difference Fourier synthesis showed features in the range of $\Delta\rho_{max}$ = 0.416 e$^-$/Å^3 to $\Delta\rho_{min}$ = −0.266 e$^-$/Å^3 which were deemed of no chemical significance. Molecular diagrams were generated using ORTEP-III[39] and POV-Ray.[40] X-ray structural data has been deposited with the CCDC.[41]

Acknowledgment. This material is based upon work supported by the National Science Foundation under Grant No. CHE-0616555 (to T.D.L.), the Camille and Henry Dreyfus Foundation, and the Petroleum Research Fund, administered by

(34) (a) Bruker *SMART CCD software package, version 5.630*; Bruker Advanced X-ray Solutions: Madison, WI, 1997−2002. (b) Bruker *SAINT+ Integration Software for Single Crystal Data frames - h,k,l, intensity, version 6.45*; Bruker Advanced X-ray Solutions: Madison, WI, 2003. (c) Bruker *SADABS-Empirical absorption correction produces*; Bruker Advanced X-ray Solutions: Madison, WI, 2003.

(35) McArdle, P. *J. Appl. Crystallogr.* **1996**, *29*, 306.

(36) Farrugia, L. J. *J. Appl. Crystallogr.* **1999**, *32*, 837−838.

(37) Burla, M. C.; Caliandro, R.; Camalli, M.; Carrozzini, B.; Cascarano, G. L.; De Caro, L.; Giacovazzo, C.; Polidori, G.; Spagna, R. *J. Appl. Crystallogr.* **2005**, *38*, 381−388.

(38) Sheldrick, G. M., *SHELX-97, Programs for Crystal Structure Analysis (Release 97−2)*, Institüt für Anorganische Chemie der Universität, Tammanstrasse 4, D-3400 Göttingen, Germany, 1998.

(39) Farrugia, L. J. *J. Appl. Crystallogr.* **1997**, *30*, 565.

(40) Persistence of Vision Team, 2006, www.povray.org.

(41) Crystallographic data (excluding structure factors) for **16a** has been deposited with the Cambridge Crystallographic Data Center as supplementary publication number CCDC 650546. Copies of this data can be obtained, free of charge, on application to CCDC, 12 Union Road, Cambridge CB2 IEZ, UK [fax: +44 (0)12233 336033 or e-mail: deposit@ccdc.cam.ac.uk].

the American Chemical Society. G.M.F. also gratefully acknowledges the National Science Foundation (Grant No. CHE-0348158) for support. We thank Dr. Matthias Zeller and the Youngstown State University Structure & Chemical Instrumentation Facility for collecting the low-temperature CCD X-ray data.

Supporting Information Available: Synthetic procedures for **13**−**15**, crystallographic data for **16a** (CIF), and copies of the UV−vis, IR, ^{1}H NMR, and ^{13}C NMR spectra for selected compounds. This material is available free of charge via the Internet at http://pubs.acs.org.

JO701523S